ENERGY NORM A-POSTERIORI ERROR ESTIMATION FOR HP-ADAPTIVE DISCONTINUOUS GALERKIN METHODS FOR ELLIPTIC PROBLEMS IN THREE DIMENSIONS

LIANG ZHU*, STEFANO GIANI†, PAUL HOUSTON‡, AND DOMINIK SCHÖTZAU §

Abstract. We develop the energy norm a-posteriori error estimation for *hp*-version discontinuous Galerkin (DG) discretizations of elliptic boundary-value problems on 1-irregularly, isotropically refined affine hexahedral meshes in three dimensions. We derive a reliable and efficient indicator for the errors measured in terms of the natural energy norm. The ratio of the efficiency and reliability constants is independent of the local mesh sizes and weakly depending on the polynomial degrees. In our analysis we make use of an *hp*-version averaging operator in three dimensions, which we explicitly construct and analyze. We use our error indicator in an *hp*-adaptive refinement algorithm and illustrate its practical performance in a series of numerical examples. Our numerical results indicate that exponential rates of convergence are achieved for problems with smooth solutions, as well as for problems with isotropic corner singularities.

1. Introduction. In this paper we develop the energy norm a-posteriori error estimation for *hp*-adaptive discontinuous Galerkin (DG) discretizations of the following model diffusion equation in three dimensions:

$$\begin{aligned} -\Delta u &= f(x) \qquad \text{in } \Omega \subset \mathbb{R}^3, \\ u &= 0 \qquad \text{on } \Gamma. \end{aligned} \tag{1.1}$$

Here, Ω is a bounded Lipschitz polyhedron in $\mathbb{R}^3$ with boundary $\Gamma = \partial\Omega$. The right-hand side $f(x)$ is a given function in $L^2(\Omega)$. The standard weak formulation of (1.1) is to find $u \in H^1_0(\Omega)$ such that

$$A(u,v) \equiv \int_\Omega \nabla u \cdot \nabla v \, dx = \int_\Omega f v \, dx \qquad \forall\, v \in H^1_0(\Omega). \tag{1.2}$$

DG methods are ideally suited for realizing *hp*-adaptivity for second-order boundary-value problems, an advantage that has been noted early on in the recent development of these methods; see, for example, [6, 11, 17, 25, 26, 30] and the references therein. Indeed, working with discontinuous finite element spaces easily facilitates the use of variable polynomial degrees and local mesh refinement techniques on possibly irregularly refined meshes – the two key ingredients for *hp*-adaptive algorithms.

The development of energy-norm error estimation for *hp*-adaptive DG methods for elliptic boundary-value problems was initiated in [16] where a residual-based *hp*-version error estimator was derived for regular meshes of triangular and quadrilateral elements on two-dimensional domains. It was verified numerically that the resulting *hp*-adaptive algorithm achieves exponential rates of convergence for problems with piecewise smooth data. In [21], a similar approach was presented for quasi-linear second-order problems in two dimensions. By using an underlying auxiliary mesh,

*Mathematics Department, University of British Columbia, Vancouver, BC, V6T 1Z2, Canada (zhuliang@math.ubc.ca).

†School of Mathematical Sciences, University of Nottingham, University Park, Nottingham, NG7 2RD, UK (stefano.giani@nottingham.ac.uk).

‡School of Mathematical Sciences, University of Nottingham, University Park, Nottingham, NG7 2RD, UK (paul.houston@nottingham.ac.uk).

§Mathematics Department, University of British Columbia, Vancouver, BC, V6T 1Z2, Canada (schoetzau@math.ubc.ca).

it was possible to also analyze the case of irregular meshes. Another technique to deal with irregular meshes was proposed in [32] where *hp*-version a-posteriori error estimates for two-dimensional convection-diffusion equations were derived that are robust in the Péclet number of the problem.

In this paper, we extend the two-dimensional analysis presented in [16] to 1-irregularly, isotropically refined affine hexahedral meshes in three space dimensions. We propose an energy norm error estimator which gives rise to global upper and local lower bounds of the error measured in the natural DG energy norm. As in [16], the ratio of these error bounds is independent of the local mesh sizes and weakly depends on the local polynomial degrees. Crucial in our analysis is the use of an averaging operator which allows us to approximate a discontinuous finite element function by a continuous one. Operators of this type were originally introduced in [22] for the energy norm a-posteriori error analysis of DG methods for elliptic problems. The same operators have been employed in the papers [9, 15, 16, 21, 28, 32], both for *h*- and *hp*-version DG methods.

Here, we follow the approach of [32] and extend the analysis there to three space dimensions. By doing so, we also obtain an optimal L^2-norm error bound for the averaging operator on irregular meshes which is of interest on its own. We use our estimators as error indicators in *hp*-adaptive computations and present a set of numerical experiments. We first test the resulting algorithms for problems with smooth solutions. Then we also show the performance of our method for a problem in the classical Fichera polyhedron, with a solution that has an isotropic singularity at the reentrant corner. In both cases, our numerical results indicate that exponential rates of convergence are achieved with respect to the number of degrees of freedom.

We emphasize that our analysis and techniques of proof are valid only for isotropically refined elements. In light of the *hp*-version a-priori error analysis for elliptic boundary-value problems presented in [27], anisotropic refinement is essential for resolving edge and edge-corner singularities with exponential rates of convergence. The extension of our results to anisotropic elements (and anisotropic polynomial spaces) remains an open question and is the subject of current research.

The outline of the rest of this article is as follows. In Section 2, we introduce the *hp*-adaptive DG discretization of the model problem stated in (1.1). In Section 3, we present our energy norm a-posteriori error estimate and discuss its reliability and local efficiency. The reliability proof shall be presented in Section 4. As an analysis tool, we use a new *hp*-version averaging operator that is analyzed in Section 5. In Section 6, we present a series of numerical tests that verify the theoretical results. Finally, in Section 7, we end with some concluding remarks.

2. Discontinuous Galerkin discretization of a diffusion problem. In this section, we introduce an *hp*-version interior penalty DG finite element method for the discretization of (1.1).

2.1. Meshes and traces. Throughout, we assume that the computational domain Ω can be partitioned into shape-regular and affine sequences of meshes $\mathcal{T} = \{K\}$ of hexahedra K. Each element $K \in \mathcal{T}$ is the image of the cube $\widehat{K} = (-1,1)^3$ under an affine elemental mapping $T_K : \widehat{K} \to K$. As usual, we denote by h_K the diameter of K. We store the elemental diameters in the mesh size vector $\underline{h} = \{ h_K : K \in \mathcal{T} \}$.

For an element $K \in \mathcal{T}$, we make use of the following sets of elemental faces: the set $\mathcal{F}(K)$ consists of the six elemental faces of K. We further denote by $\mathcal{F}_B(K)$ the elemental faces of K that lie on Γ, and by $\mathcal{F}_I(K)$ the set of interior faces; thereby, we

have that $\mathcal{F}(K) = \mathcal{F}_B(K) \cup \mathcal{F}_I(K)$.

In order to be able to deal with irregular meshes, we also need to define the faces of a mesh $\mathcal{T}$. We refer to F as an interior mesh face of $\mathcal{T}$ if $F = \partial K \cap \partial K'$ for two neighboring elements $K, K' \in \mathcal{T}$ whose intersection has a positive surface measure. The set of all interior mesh faces is denoted by $\mathcal{F}_I(\mathcal{T})$. Analogously, if the intersection $F = \partial K \cap \Gamma$ of the boundary of an element $K \in \mathcal{T}$ and Γ is of positive surface measure, we refer to F as a boundary mesh face of $\mathcal{T}$. The set of all boundary mesh faces of $\mathcal{T}$ is denoted by $\mathcal{F}_B(\mathcal{T})$ and we set $\mathcal{F}(\mathcal{T}) = \mathcal{F}_I(\mathcal{T}) \cup \mathcal{F}_B(\mathcal{T})$. The diameter of a face F is denoted by h_F.

We allow for 1-irregularly refined meshes $\mathcal{T}$ defined as follows. Let K be an element of $\mathcal{T}$ and F an elemental face in $\mathcal{F}(K)$. Then F may contain at most one hanging node located in the center of F and at most one hanging node in the middle of each elemental edge of F. That is, we have that F is either a mesh face belonging to $\mathcal{F}(\mathcal{T})$ or F can be written as $F = \cup_{i=1}^{4} F_i$, with four mesh faces $F_i \in \mathcal{F}(\mathcal{T})$, $i = 1, \ldots, 4$, of diameter $h_{F_i} = h_F/2$, respectively.

Next, let us define the jumps and averages of piecewise smooth functions across faces of the mesh $\mathcal{T}$. To that end, let the interior face $F \in \mathcal{F}_I(\mathcal{T})$ be shared by two neighboring elements K and K^{e} where the superscript e stands for "exterior". For a piecewise smooth function v, we denote by $v|_F$ the trace on F taken from inside K, and by $v^{\mathrm{e}}|_F$ the one taken from inside K^{e}. The average and jump of v across the face F are then defined as

$$\{\!\{v\}\!\} = \frac{1}{2}(v|_F + v^{\mathrm{e}}|_F), \qquad [\![v]\!] = v|_F \, \underline{n}_K + v^{\mathrm{e}}|_F \, \underline{n}_{K^{\mathrm{e}}}.$$

Here, $\underline{n}_K$ and $\underline{n}_{K^{\mathrm{e}}}$ denote the unit outward normal vectors on the boundary of elements K and K^{e}, respectively. Similarly, if $\underline{q}$ is piecewise smooth vector field, its average and (normal) jump across F are given by

$$\{\!\{\underline{q}\}\!\} = \frac{1}{2}\left(\underline{q}|_F + \underline{q}^{\mathrm{e}}|_F\right), \qquad [\![\underline{q}]\!] = \underline{q}|_F \cdot \underline{n}_K + \underline{q}^{\mathrm{e}}|_F \cdot \underline{n}_{K^{\mathrm{e}}}.$$

On a boundary face $F \in \mathcal{F}_B(\mathcal{T})$, we accordingly set $\{\!\{\underline{q}\}\!\} = \underline{q}$ and $[\![v]\!] = v\underline{n}$, with $\underline{n}$ denoting the unit outward normal vector on Γ. The other trace operators will not be used on boundary faces and are thereby left undefined.

2.2. Finite element spaces. We begin by introducing polynomial spaces on elements and faces. To that end, let $K \in \mathcal{T}$ be an element. We set

$$\mathcal{Q}_p(K) = \{\, v \,:\, K \to \mathbb{R} \,:\, v \circ T_K \in \mathcal{Q}_p(\widehat{K}) \,\}, \tag{2.1}$$

with $\mathcal{Q}_p(\widehat{K})$ denoting the set of tensor product polynomials on the reference element $\widehat{K}$ of degree less than or equal to p in each coordinate direction on $\widehat{K}$. In addition, if $F \in \mathcal{F}(K)$ is a face of K and $\widehat{F}$ the corresponding one on the reference element $\widehat{K}$, we define

$$\mathcal{Q}_p(F) = \{\, v \,:\, F \to \mathbb{R} \,:\, v \circ T_K|_F \in \mathcal{Q}_p(\widehat{F}) \,\}, \tag{2.2}$$

where $\mathcal{Q}_p(\widehat{F})$ denotes the set of tensor product polynomials on $\widehat{F}$ of degree less than or equal to p in each coordinate direction on $\widehat{F}$.

To define hp-version finite element spaces, we assign a polynomial degree $p_K \geq 1$ with each element K of the mesh $\mathcal{T}$. We then introduce the degree vector $\underline{p} = \{\, p_K \,:$

$K \in \mathcal{T}\}$. We assume that $\underline{p}$ is of bounded local variation, that is, there is a constant $\varrho \geq 1$, independent of the mesh $\mathcal{T}$ sequence under consideration, such that

$$\varrho^{-1} \leq p_K/p_{K'} \leq \varrho \tag{2.3}$$

for any pair of neighboring elements $K, K' \in \mathcal{T}$. For a mesh face $F \in \mathcal{F}(\mathcal{T})$, we introduce the face polynomial degree p_F by

$$p_F = \begin{cases} \max\{p_K, p_{K'}\}, & \text{if } F = \partial K \cap \partial K' \in \mathcal{F}_I(\mathcal{T}), \\ p_K, & \text{if } F = \partial K \cap \Gamma \in \mathcal{F}_B(\mathcal{T}). \end{cases} \tag{2.4}$$

For a partition $\mathcal{T}$ of Ω and a polynomial degree vector $\underline{p}$ on $\mathcal{T}$, we define the *hp*-version DG finite element space by

$$S_{\underline{p}}(\mathcal{T}) = \{\, v \in L^2(\Omega) \,:\, v|_K \in \mathcal{Q}_{p_K}(K),\ K \in \mathcal{T}\,\}. \tag{2.5}$$

2.3. Interior penalty discretization. We now consider the following interior penalty DG discretization for the numerical approximation of the diffusion problem (1.1): find $u_{hp} \in S_{\underline{p}}(\mathcal{T})$ such that

$$A_{hp}(u_{hp}, v) = \int_\Omega f v\, dx \qquad \forall\, v \in S_{\underline{p}}(\mathcal{T}). \tag{2.6}$$

The bilinear form $A_{hp}(u, v)$ is given by

$$\begin{aligned} A_{hp}(u,v) = &\sum_{K\in\mathcal{T}} \int_K \nabla u \cdot \nabla v\, dx - \sum_{F\in\mathcal{F}(\mathcal{T})} \int_F \Big(\{\!\{\nabla u\}\!\} \cdot [\![v]\!] + \{\!\{\nabla v\}\!\} \cdot [\![u]\!] \Big)\, ds \\ &+ \sum_{F\in\mathcal{F}(\mathcal{T})} \frac{\gamma p_F^2}{h_F} \int_F [\![u]\!] \cdot [\![v]\!]\, ds, \end{aligned}$$

where the gradient operator ∇ is defined elementwise. The parameter $\gamma > 0$ is the interior penalty parameter. The method in (2.6) is a straightforward extension of the classical (symmetric) interior penalty method introduced in [4, 24] to the context of the *hp*-version finite element method; see also [5, 17, 30] and the references therein.

REMARK 2.1. *The stability and well-posedness of the DG method (2.6) follow from the same arguments as those employed in [30, Proposition 3.8] used to analyze the scheme in two-dimensions: there is a threshold parameter $\gamma_0 > 0$, independent of $\underline{h}$ and $\underline{p}$, such that for $\gamma \geq \gamma_0$ the formulation (2.6) possesses a unique solution $u_{hp} \in S_{\underline{p}}(\mathcal{T})$.*

3. Energy norm a-posteriori error estimates. In this section, we present and discuss our main results.

3.1. Energy norm and residuals. We measure the error in the following energy norm associated with the DG formulation (2.6):

$$\|\, u \,\|^2_{\mathrm{E},\mathcal{T}} = \sum_{K\in\mathcal{T}} \|\nabla u\|^2_{L^2(K)} + \sum_{F\in\mathcal{F}(\mathcal{T})} \frac{\gamma p_F^2}{h_F} \|[\![u]\!]\|^2_{L^2(F)}. \tag{3.1}$$

To introduce our energy norm indicator, let $u_{hp} \in S_{\underline{p}}(\mathcal{T})$ be the DG approximation obtained by (2.6). Moreover, we denote by f_{hp} a piecewise polynomial approximation in $S_{\underline{p}}(\mathcal{T})$ of the right-hand side f. For each element $K \in \mathcal{T}$, we introduce the

following local error indicator η_K which is given by the sum of the three terms

$$\eta_K^2 = \eta_{R_K}^2 + \eta_{F_K}^2 + \eta_{J_K}^2. \tag{3.2}$$

The first term η_{R_K} is the interior residual defined by

$$\eta_{R_K}^2 = p_K^{-2} h_K^2 \| f_{hp} + \Delta u_{hp} \|_{L^2(K)}^2.$$

The second term η_{F_K} is the face residual given by

$$\eta_{F_K}^2 = \frac{1}{2} \sum_{F \in \mathcal{F}_I(K)} p_F^{-1} h_F \| [\![\nabla u_{hp}]\!] \|_{L^2(F)}^2.$$

The last residual η_{J_K} measures the jumps of the approximate solution u_{hp} and is defined as

$$\eta_{J_K}^2 = \frac{1}{2} \sum_{F \in \mathcal{F}_I(K)} \frac{\gamma^2 p_F^3}{h_F} \| [\![u_{hp}]\!] \|_{L^2(F)}^2 + \sum_{F \in \mathcal{F}_B(K)} \frac{\gamma^2 p_F^3}{h_F} \| [\![u_{hp}]\!] \|_{L^2(F)}^2.$$

We also introduce the local data approximation term

$$\Theta_K^2 = p_K^{-2} h_K^2 \| f - f_{hp} \|_{L^2(K)}^2. \tag{3.3}$$

Summing up the local error indicators, we introduce the global a-posteriori error estimator

$$\eta = \left(\sum_{K \in \mathcal{T}} \eta_K^2 \right)^{\frac{1}{2}}. \tag{3.4}$$

Similarly, we define the global data approximation term

$$\Theta = \left(\sum_{K \in \mathcal{T}} \Theta_K^2 \right)^{\frac{1}{2}}. \tag{3.5}$$

3.2. Reliability. Our first theorem states that, up to a constant and to data approximation, the estimator η in (3.4) gives rise to a reliable a-posteriori error bound. In this result and in the sequel, we shall use the symbols $\lesssim$ and $\gtrsim$ to denote bounds that are valid up to positive constants independent of $\underline{h}$ and $\underline{p}$.

THEOREM 3.1. *Let u be the solution of (1.1) and $u_{hp} \in S_{\underline{p}}(\mathcal{T})$ its DG approximation obtained by (2.6) with $\gamma \geq \gamma_0$. Let the error estimator η be defined by (3.4) and the data approximation error Θ by (3.5). Then we have the a-posteriori error bound*

$$\| u - u_{hp} \|_{\mathrm{E},\mathcal{T}} \lesssim \eta + \Theta.$$

The detailed proof of Theorem 3.1 will be given in Section 4. It is similar to the one given in [32] for two-dimensional convection-diffusion equations. Crucial in our proof, however, is the use of a three-dimensional averaging operator, whose *hp*-version approximation properties will be introduced in Theorem 4.1 and proven in Section 5.

REMARK 3.2. *As for the two-dimensional cases analyzed in [21, 32], the penalization of the jump terms in the interior penalty form $A_{hp}(u,v)$ is of the order $p_F^2 h_F^{-1}$ on each face, while the corresponding weight in the jump residual η_{J_K} is of the different order $p_F^3 h_F^{-1}$. This suboptimality with respect to the powers of p_F is due to the possible presence of hanging nodes in the underlying mesh $\mathcal{T}$. Indeed, on meshes without irregular nodes, Theorem 3.1 holds true with the following (optimal) jump residual:*

$$\widehat{\eta}_{J_K}^2 = \frac{1}{2} \sum_{F \in \mathcal{F}_I(K)} \frac{\gamma^2 p_F^2}{h_F} \| [\![u_{hp}]\!] \|_{L^2(F)}^2 + \sum_{F \in \mathcal{F}_B(K)} \frac{\gamma^2 p_F^2}{h_F} \| [\![u_{hp}]\!] \|_{L^2(F)}^2;$$

see also Remark 4.3 below. The associated estimator $\widehat{\eta}$ is then given by

$$\widehat{\eta}^2 = \sum_{K \in \mathcal{T}} \widehat{\eta}_K^2 \qquad \text{with} \qquad \widehat{\eta}_K^2 = \eta_{R_K}^2 + \eta_{F_K}^2 + \widehat{\eta}_{J_K}^2. \tag{3.6}$$

Our numerical experiments in Section 6 indicate that the indicators η and $\widehat{\eta}$ yield almost identical results on 1-irregular meshes.

3.3. Efficiency. In our next result, we present a local lower bound for the error measured in the energy norm. As for many residual-based *hp*-version a-posteriori error estimates, reliability and efficiency bounds, which are uniform in $\underline{p}$, are not readily available; cf. [16, 23] and the references therein. We thus restrict ourselves to stating a weakly p-dependent local lower bound for η_K defined in (3.2). We note that our numerical results indicate that exponential rates of convergence are obtained for both smooth and non-smooth solutions; in this context, the p-suboptimality is less relevant.

For an element $K \in \mathcal{T}$, we introduce the patch of neighboring elements as

$$w_K = \{K' \in \mathcal{T} \,:\, \partial K' \cap \partial K \in \mathcal{F}(\mathcal{T})\}. \tag{3.7}$$

The local energy norm over w_K is defined by

$$\| u \|_{\mathrm{E},w_K}^2 = \sum_{K' \in w_K} \| \nabla u \|_{L^2(K')}^2 + \sum_{F \in \mathcal{F}(K)} \frac{\gamma p_F^2}{h_F} \| [\![u]\!] \|_{L^2(F)}^2. \tag{3.8}$$

Similarly, we set

$$\Theta_{w_K} = \left(\sum_{K' \in w_K} \Theta_{K'}^2 \right)^{1/2}. \tag{3.9}$$

With this notation the following result holds.

THEOREM 3.3. *Let u be the solution of (1.1) and $u_{hp} \in S_{\underline{p}}(\mathcal{T})$ its DG approximation obtained by (2.6) with $\gamma \geq \gamma_0$. Let the local error estimators η_K be defined by (3.2) and the local data approximation error Θ_K by (3.3). Then, for any $\delta \in (0, \frac{1}{2})$, we have the local upper bound*

$$\eta_K \lesssim p_K^{\delta+1} \| u - u_{hp} \|_{\mathrm{E},w_K} + p_K^{2\delta+\frac{1}{2}} \Theta_{w_K}.$$

The proof of Theorem 3.3 follows in an analogous manner to the proofs of efficiency derived in [16, 21, 23, 32] for two-dimensional problems. Thereby, for the sake of brevity, we omit the proof of Theorem 3.3 and refer the reader to [31] for details.

REMARK 3.4. *As in the two-dimensional case considered in [16], our error estimator can be extended to the Poisson problem with the inhomogeneous boundary condition $u = g$ on Γ for $g \in H^{1/2}(\Gamma)$. In this case, the local error indicators η_K have to be modified by redefining the jump estimators η_{J_K} as*

$$\eta_{J_K}^2 = \frac{1}{2} \sum_{F \in \mathcal{F}_I(K)} \frac{\gamma^2 p_F^3}{h_F} \|[\![u_{hp}]\!]\|_{L^2(F)}^2 + \sum_{F \in \mathcal{F}_B(K)} \frac{\gamma^2 p_F^3}{h_F} \|u_{hp} - g_{hp}\|_{L^2(F)}^2,$$

where g_{hp} is a polynomial approximation of the boundary datum g. In this setting, Theorem 3.1 and Theorem 3.3 still hold with the inclusion of an additional data-oscillation term on the boundary; see [16] for details.

4. Proof of Theorem 3.1. In this section, we present the proof of Theorem 3.1. To this end, we proceed in the following steps.

4.1. Edges and nodes. We begin by introducing the following sets associated with nodes. We denote by $\mathcal{N}(K)$ the set of eight vertices of an element $K \in \mathcal{T}$, and by $\mathcal{N}(F)$ the set of the four vertices of a face F in $\mathcal{F}(\mathcal{T})$. We then introduce the set of all mesh nodes by

$$\mathcal{N}(\mathcal{T}) = \bigcup_{K \in \mathcal{T}} \mathcal{N}(K).$$

We write $\mathcal{N}(\mathcal{T}) = \mathcal{N}_I(\mathcal{T}) \cup \mathcal{N}_B(\mathcal{T})$, where $\mathcal{N}_I(\mathcal{T})$ and $\mathcal{N}_B(\mathcal{T})$ are the sets of interior and boundary mesh nodes, respectively.

Next, we introduce the following sets of edges. We denote $\mathcal{E}(K)$ the set of the twelve elemental edges of an element $K \in \mathcal{T}$, and by $\mathcal{E}(F)$ the set of the four edges of a mesh face $F \in \mathcal{F}(\mathcal{T})$. We call E an edge of the mesh $\mathcal{T}$ if $E = \partial F \cap \partial F'$ is a line segment given by the intersection of two faces F, F' in $\mathcal{F}(\mathcal{T})$ in such a way that its midpoint is not a mesh node of $\mathcal{N}(\mathcal{T})$. We denote by $\mathcal{E}(\mathcal{T})$ the set of all mesh edges of $\mathcal{T}$. The length of an edge E is denoted by h_E.

4.2. Auxiliary meshes. As in [32], we shall make use of an auxiliary 1-irregular mesh $\widetilde{\mathcal{T}}$ of affine hexahedra. We construct the auxiliary mesh $\widetilde{\mathcal{T}}$ from the mesh $\mathcal{T}$ as follows. Let $K \in \mathcal{T}$. If all twelve elemental edges are edges of the mesh $\mathcal{T}$, that is, if $\mathcal{E}(K) \subseteq \mathcal{E}(\mathcal{T})$ (in this case, we have also $\mathcal{F}(K) \subseteq \mathcal{F}(\mathcal{T})$), we leave K untouched. Otherwise, at least one of the elemental edges of K contains a hanging node. In this case, we replace K by the eight hexahedral elements obtained from bisecting the elemental edges of K; see [32] for an illustration of the analogous construction in two dimensions. Clearly, the mesh $\widetilde{\mathcal{T}}$ is a refinement of $\mathcal{T}$; it is also shape-regular and 1-irregular. More importantly, the hanging nodes of $\mathcal{T}$ are not hanging nodes of $\widetilde{\mathcal{T}}$ anymore. In the following, we shall write $\mathcal{R}(K)$ for the elements in $\widetilde{\mathcal{T}}$ that are inside K. That is, if K is unrefined, we have $\mathcal{R}(K) = \{K\}$. Otherwise $\mathcal{R}(K)$ consists of eight newly created elements.

We denote by $\mathcal{F}_R(\mathcal{T})$ the set of mesh faces in $\mathcal{F}(\mathcal{T})$ that have been refined in the construction of $\widetilde{\mathcal{T}}$. Furthermore, we denote by $\mathcal{F}_H(\mathcal{T})$ the set of faces in $\mathcal{F}_R(\mathcal{T})$ that have at least one hanging node of $\mathcal{T}$ on their edges, and by $\mathcal{F}_N(\mathcal{T})$ the ones that have no hanging nodes of $\mathcal{T}$ on their edges. The sets of nodes, edges and faces of the auxiliary mesh $\widetilde{\mathcal{T}}$ are denoted by $\mathcal{N}(\widetilde{\mathcal{T}})$, $\mathcal{E}(\widetilde{\mathcal{T}})$ and $\mathcal{F}(\widetilde{\mathcal{T}})$, respectively; these sets are defined in an analogous manner to the corresponding sets introduced for the mesh $\mathcal{T}$.

We then define the following subsets of $\mathcal{N}(\widetilde{\mathcal{T}})$, $\mathcal{E}(\widetilde{\mathcal{T}})$ and $\mathcal{F}(\widetilde{\mathcal{T}})$:

$$\mathcal{N}_A(\widetilde{\mathcal{T}}) = \{\, \widetilde{\nu} \in \mathcal{N}(\widetilde{\mathcal{T}}) \,:\, \exists K \in \mathcal{T} \text{ such that } \widetilde{\nu} \text{ is inside } K \,\},$$
$$\mathcal{E}_A(\widetilde{\mathcal{T}}) = \{\, \widetilde{E} \in \mathcal{E}(\widetilde{\mathcal{T}}) \,:\, \exists K \in \mathcal{T} \text{ such that } \widetilde{E} \text{ is inside } K \,\},$$
$$\mathcal{F}_A(\widetilde{\mathcal{T}}) = \{\, \widetilde{F} \in \mathcal{F}(\widetilde{\mathcal{T}}) \,:\, \exists K \in \mathcal{T} \text{ such that } \widetilde{F} \text{ is inside } K \,\}.$$

We then introduce the following auxiliary DG finite element space on the mesh $\widetilde{\mathcal{T}}$:

$$S_{\underline{\widetilde{p}}}(\widetilde{\mathcal{T}}) = \{\, v \in L^2(\Omega) \,:\, v|_{\widetilde{K}} \circ T_{\widetilde{K}} \in \mathcal{Q}_{p_{\widetilde{K}}}(\widehat{K}),\ \widetilde{K} \in \widetilde{\mathcal{T}} \,\},$$

where the auxiliary polynomial degree vector $\underline{\widetilde{p}}$ is defined by $p_{\widetilde{K}} = p_K$ for $\widetilde{K} \in \mathcal{R}(K)$ and $T_{\widetilde{K}}$ is the affine mapping from $\widehat{K}$ onto $\widetilde{K}$. We clearly have the following inclusion:

$$S_{\underline{p}}(\mathcal{T}) \subseteq S_{\underline{\widetilde{p}}}(\widetilde{\mathcal{T}}). \tag{4.1}$$

In analogy with (3.1), the energy norm associated with $\widetilde{\mathcal{T}}$ is defined by

$$\| u \|^2_{\mathrm{E},\widetilde{\mathcal{T}}} = \sum_{\widetilde{K} \in \widetilde{\mathcal{T}}} \|\nabla u\|^2_{L^2(\widetilde{K})} + \sum_{\widetilde{F} \in \mathcal{F}(\widetilde{\mathcal{T}})} \frac{\gamma p^2_{\widetilde{F}}}{h_{\widetilde{F}}} \|[\![u]\!]\|^2_{L^2(\widetilde{F})}, \tag{4.2}$$

where the auxiliary face polynomial degrees $p_{\widetilde{F}}$ for the jump terms over $\widetilde{\mathcal{T}}$ are defined as in (2.4), but using the auxiliary degrees $p_{\widetilde{K}}$.

4.3. Averaging operator. Our analysis is based on an *hp*-version averaging operator that allows us to approximate discontinuous functions by continuous ones. Analogous operators are used in the *hp*-version approaches presented in [9, 16, 21, 32]. For the *h*-version of the DG method, we also refer the reader to [13, 22] and the references therein. To state our result, let $S^c_{\underline{\widetilde{p}}}(\widetilde{\mathcal{T}})$ be the conforming subspace of $S_{\underline{\widetilde{p}}}(\widetilde{\mathcal{T}})$ given by

$$S^c_{\underline{\widetilde{p}}}(\widetilde{\mathcal{T}}) = S_{\underline{\widetilde{p}}}(\widetilde{\mathcal{T}}) \cap H^1_0(\Omega). \tag{4.3}$$

THEOREM 4.1. *There exists an averaging operator* $I_{hp} : S_{\underline{p}}(\mathcal{T}) \to S^c_{\underline{\widetilde{p}}}(\widetilde{\mathcal{T}})$ *that satisfies*

$$\sum_{\widetilde{K} \in \widetilde{\mathcal{T}}} \|\nabla(v - I_{hp}v)\|^2_{L^2(\widetilde{K})} \lesssim \sum_{F \in \mathcal{F}(\mathcal{T})} p^2_F h_F^{-1} \|[\![v]\!]\|^2_{L^2(F)}, \tag{4.4}$$

$$\sum_{\widetilde{K} \in \widetilde{\mathcal{T}}} \|v - I_{hp}v\|^2_{L^2(\widetilde{K})} \lesssim \sum_{F \in \mathcal{F}(\mathcal{T})} p_F^{-2} h_F \|[\![v]\!]\|^2_{L^2(F)}. \tag{4.5}$$

The explicit construction of I_{hp} and the detailed proof of properties (4.4)–(4.5) are presented in Section 5.

REMARK 4.2. *The result in Theorem 4.1 generalizes several hp-version approximation results of the same type to three dimensions. The analyses in [16, 21] showed the* H^1*-norm estimate (4.4) on two-dimensional regular and irregular meshes, respectively. In [9, Lemma 3.2], both estimates in (4.4) and (4.5) were proven for regular two-dimensional meshes and a fixed polynomial degree. In [32], these results have been extended to two-dimensional 1-irregular meshes and variable polynomial degrees.*

REMARK 4.3. *We emphasize that for partitions with no irregular nodes, the auxiliary mesh* $\widetilde{\mathcal{T}}$ *coincides with* $\mathcal{T}$*. In this case, Theorem 4.1 holds true directly on the original mesh* $\mathcal{T}$*.*

4.4. Proof of Theorem 3.1. To prove Theorem 3.1, we follow [16, 28] and decompose the DG solution u_{hp} into a conforming part and a remainder:

$$u_{hp} = u_{hp}^c + u_{hp}^r,$$

where $u_{hp}^c = I_{hp} u_{hp} \in S^c_{\underline{p}}(\widetilde{\mathcal{T}}) \subset H_0^1(\Omega)$ is defined using the averaging operator I_{hp} in Theorem 4.1. The remainder u_{hp}^r is given by $u_{hp}^r = u_{hp} - u_{hp}^c \in S_{\underline{p}}(\widetilde{\mathcal{T}})$. Analogously to [32, Lemma 4.4], one can show that

$$\| u - u_{hp} \|_{\mathrm{E},\mathcal{T}} \lesssim \| u - u_{hp} \|_{\mathrm{E},\widetilde{\mathcal{T}}}.$$

Therefore, by the triangle inequality,

$$\| u - u_{hp} \|_{\mathrm{E},\mathcal{T}} \lesssim \| u - u_{hp}^c \|_{\mathrm{E},\widetilde{\mathcal{T}}} + \| u_{hp}^r \|_{\mathrm{E},\widetilde{\mathcal{T}}}.$$

Finally, since $u - u_{hp}^c \in H_0^1(\Omega)$, we have $\| u - u_{hp}^c \|_{\mathrm{E},\mathcal{T}} = \| u - u_{hp}^c \|_{\mathrm{E},\widetilde{\mathcal{T}}}$. As the starting point of our proof, we thus obtain the following inequality:

$$\| u - u_{hp} \|_{\mathrm{E},\mathcal{T}} \lesssim \| u - u_{hp}^c \|_{\mathrm{E},\mathcal{T}} + \| u_{hp}^r \|_{\mathrm{E},\widetilde{\mathcal{T}}}. \tag{4.6}$$

We first show that $\| u_{hp}^r \|_{\mathrm{E},\widetilde{\mathcal{T}}}$ in (4.6) can be bounded by the error estimator η.

LEMMA 4.4. *Under the foregoing assumptions, the following upper bound holds*

$$\| u_{hp}^r \|_{\mathrm{E},\widetilde{\mathcal{T}}} \lesssim \eta.$$

Proof. Recall from (4.2) that

$$\| u_{hp}^r \|^2_{\mathrm{E},\widetilde{\mathcal{T}}} = \sum_{\widetilde{K} \in \widetilde{\mathcal{T}}} \|\nabla u_{hp}^r\|^2_{L^2(\widetilde{K})} + \sum_{\widetilde{F} \in \mathcal{F}(\widetilde{\mathcal{T}})} \frac{\gamma p_{\widetilde{F}}^2}{h_{\widetilde{F}}} \|[\![u_{hp}^r]\!]\|^2_{L^2(\widetilde{F})}.$$

Since $u_{hp} \in S_{\underline{p}}(\mathcal{T})$ and $[\![u_{hp}^r]\!]|_F = [\![u_{hp}]\!]|_F$ for all $F \in \mathcal{F}(\widetilde{\mathcal{T}})$, an argument similar to [32, Lemma 4.3] allows us to bound the jump terms by

$$\sum_{\widetilde{F} \in \mathcal{F}(\widetilde{\mathcal{T}})} \frac{\gamma p_{\widetilde{F}}^2}{h_{\widetilde{F}}} \|[\![u_{hp}^r]\!]\|^2_{L^2(\widetilde{F})} \lesssim \gamma^{-1} \sum_{F \in \mathcal{F}(\mathcal{T})} \frac{\gamma^2 p_F^2}{h_F} \|[\![u_{hp}]\!]\|^2_{L^2(F)} \lesssim \gamma^{-1} \sum_{K \in \mathcal{T}} \eta_{J_K}^2,$$

where we have also used the fact that $p_F \geq 1$. To bound the volume terms, we apply Theorem 4.1 and the last bound in the previous argument. This results in the estimate

$$\sum_{\widetilde{K} \in \widetilde{\mathcal{T}}} \|\nabla u_{hp}^r\|^2_{L^2(\widetilde{K})} \lesssim \gamma^{-2} \sum_{F \in \mathcal{F}(\mathcal{T})} \frac{\gamma^2 p_F^2}{h_F} \|[\![u_{hp}]\!]\|^2_{L^2(F)} \lesssim \gamma^{-2} \sum_{K \in \mathcal{T}} \eta_{J_K}^2.$$

This completes the proof. ∎

To bound $\| u - u_{hp}^c \|_{\mathrm{E},\mathcal{T}}$ in (4.6), we shall make use of the following two auxiliary forms:

$$D_{hp}(u,v) = \sum_{K \in \mathcal{T}} \int_K \nabla u \cdot \nabla v \, dx + \sum_{F \in \mathcal{F}(\mathcal{T})} \frac{\gamma p_F^2}{h_F} \int_F [\![u]\!] \cdot [\![v]\!] \, ds,$$

$$K_{hp}(u,v) = - \sum_{F \in \mathcal{F}(\mathcal{T})} \int_F \{\!\{ \nabla u \}\!\} \cdot [\![v]\!] \, ds - \sum_{F \in \mathcal{F}(\mathcal{T})} \int_F \{\!\{ \nabla v \}\!\} \cdot [\![u]\!] \, ds.$$

The form $D_{hp}(u,v)$ is well-defined for $u,v \in S_{\underline{p}}(\mathcal{T}) + H_0^1(\Omega)$, whereas $K_{hp}(u,v)$ is only well-defined for discrete functions $u,v \in S_{\mathbf{p}}(\mathcal{T})$. Furthermore, we have

$$A(u,v) = D_{hp}(u,v) \qquad \forall\, u,v \in H_0^1(\Omega), \tag{4.7}$$

as well as

$$A_{hp}(u,v) = D_{hp}(u,v) + K_{hp}(u,v) \qquad \forall\, u,v \in S_{\underline{p}}(\mathcal{T}). \tag{4.8}$$

We also recall the standard *hp*-version approximation result from [21, Lemma 3.7]: For any $v \in H_0^1(\Omega)$, there exists a function $v_{hp} \in S_{\underline{p}}(\mathcal{T})$ such that

$$\begin{aligned} p_K^2 h_K^{-2} \|v - v_{hp}\|_{L^2(K)}^2 &\lesssim \|\nabla v\|_{L^2(K)}^2, \\ \|\nabla(v - v_{hp})\|_{L^2(K)}^2 &\lesssim \|\nabla v\|_{L^2(K)}^2, \\ p_K h_K^{-1} \|v - v_{hp}\|_{L^2(\partial K)}^2 &\lesssim \|\nabla v\|_{L^2(K)}^2, \end{aligned} \tag{4.9}$$

for any element $K \in \mathcal{T}$.

Next, we prove the following auxiliary estimate.

LEMMA 4.5. *For any $v \in H_0^1(\Omega)$, we have*

$$\int_\Omega f(v - v_{hp})\,dx - D_{hp}(u_{hp}, v - v_{hp}) + K_{hp}(u_{hp}, v_{hp}) \lesssim (\eta + \Theta)\,|\!|\!|\, v \,|\!|\!|_{\mathrm{E},\mathcal{T}}.$$

Here, $v_{hp} \in S_{\underline{p}}(\mathcal{T})$ is the hp-version approximation of v defined in (4.9).

Proof. For notational convenience, let us set

$$T = \int_\Omega f(v - v_{hp})\,dx - D_{hp}(u_{hp}, v - v_{hp}) + K_{hp}(u_{hp}, v_{hp}).$$

By writing out the forms D_{hp} and K_{hp}, integrating by parts the volume terms and manipulating the resulting expressions, we readily obtain

$$\begin{aligned} T &= \sum_{K\in\mathcal{T}} \int_K (f + \Delta u_{hp})(v - v_{hp})\,dx - \sum_{F\in\mathcal{F}(\mathcal{T})} \frac{\gamma p_F^2}{h_F} \int_F [\![u_{hp}]\!] \cdot [\![v - v_{hp}]\!]\,ds \\ &\quad - \sum_{F\in\mathcal{F}_I(\mathcal{T})} \int_F [\![\nabla u_{hp}]\!] \{\!\{v - v_{hp}\}\!\}\,ds - \sum_{F\in\mathcal{F}(\mathcal{T})} \int_F \{\!\{\nabla v_{hp}\}\!\} \cdot [\![u_{hp}]\!]\,ds \\ &\equiv T_1 + T_2 + T_3 + T_4. \end{aligned}$$

To bound term T_1, we first add and subtract the approximation f_{hp} to f:

$$T_1 = \sum_{K\in\mathcal{T}} \int_K (f_{hp} + \Delta u_{hp})(v - v_{hp})\,dx + \sum_{K\in\mathcal{T}} \int_K (f - f_{hp})(v - v_{hp})\,dx.$$

Using the Cauchy-Schwarz inequality and the approximation properties (4.9) shows that

$$\begin{aligned} T_1 &\lesssim \Big(\sum_{K\in\mathcal{T}} \big(\eta_{R_K}^2 + \Theta_K^2\big) \Big)^{\frac{1}{2}} \Big(\sum_{K\in\mathcal{T}} p_K^2 h_K^{-2} \|v - v_{hp}\|_{L^2(K)}^2 \Big)^{\frac{1}{2}} \\ &\lesssim \Big(\sum_{K\in\mathcal{T}} \big(\eta_{R_K}^2 + \Theta_K^2\big) \Big)^{\frac{1}{2}} |\!|\!|\, v \,|\!|\!|_{\mathrm{E},\mathcal{T}}. \end{aligned}$$

For term T_2, we again exploit the Cauchy-Schwarz inequality to conclude that

$$T_2 \leq \Big(\sum_{F\in\mathcal{F}(\mathcal{T})} \gamma^2 p_F^3 h_F^{-1} \|[\![u_{hp}]\!]\|^2_{L^2(F)} \Big)^{\frac{1}{2}} \Big(\sum_{F\in\mathcal{F}(\mathcal{T})} p_F h_F^{-1} \|[\![v - v_{hp}]\!]\|^2_{L^2(F)} \Big)^{\frac{1}{2}}.$$

Thus, by the shape-regularity of the meshes, the bounded variation property (2.3) of the polynomial degrees and the approximation properties (4.9), we get the bound

$$T_2 \lesssim \Big(\sum_{K\in\mathcal{T}} \eta^2_{J_K} \Big)^{\frac{1}{2}} \| v \|_{\mathrm{E},\mathcal{T}}.$$

Similarly, term T_3 can be bounded by

$$\begin{aligned} T_3 &\leq \Big(\sum_{F\in\mathcal{F}_I(\mathcal{T})} p_F^{-1} h_F \|[\![\nabla u_{hp}]\!]\|^2_{L^2(F)} \Big)^{\frac{1}{2}} \Big(\sum_{F\in\mathcal{F}_I(\mathcal{T})} p_F h_F^{-1} \|\{\!\{v - v_{hp}\}\!\}\|^2_{L^2(F)} \Big)^{\frac{1}{2}} \\ &\lesssim \Big(\sum_{K\in\mathcal{T}} \eta^2_{F_K} \Big)^{\frac{1}{2}} \| v \|_{\mathrm{E},\mathcal{T}}. \end{aligned}$$

Finally, for term T_4, we use the Cauchy-Schwarz inequality, the shape-regularity of the meshes, and the bounded variation property (2.3) of the polynomial degrees, to obtain

$$T_4 \lesssim \gamma^{-1} \Big(\sum_{F\in\mathcal{F}(\mathcal{T})} \gamma^2 p_F^2 h_F^{-1} \|[\![u_{hp}]\!]\|^2_{L^2(F)} \Big)^{\frac{1}{2}} \Big(\sum_{K\in\mathcal{T}} p_K^{-2} h_K \|\nabla v_{hp}\|^2_{L^2(\partial K)} \Big)^{\frac{1}{2}}.$$

¿From the standard *hp*-version inverse trace inequality, see [29], we conclude that

$$T_4 \lesssim \gamma^{-1} \Big(\sum_{K\in\mathcal{T}} \eta^2_{J_K} \Big)^{\frac{1}{2}} \Big(\sum_{K\in\mathcal{T}} \|\nabla v_{hp}\|^2_{L^2(K)} \Big)^{\frac{1}{2}}.$$

¿From the approximation properties in (4.9) it follows that

$$\sum_{K\in\mathcal{T}} \|\nabla v_{hp}\|^2_{L^2(K)} \lesssim \sum_{K\in\mathcal{T}} \|\nabla(v - v_{hp})\|^2_{L^2(K)} + \sum_{K\in\mathcal{T}} \|\nabla v\|^2_{L^2(K)} \lesssim \| v \|^2_{\mathrm{E},\mathcal{T}}.$$

Hence,

$$T_4 \lesssim \gamma^{-1} \Big(\sum_{K\in\mathcal{T}} \eta^2_{J_K} \Big)^{\frac{1}{2}} \| v \|_{\mathrm{E},\mathcal{T}}.$$

The above bounds for terms T_1, T_2, T_3, and T_4 now imply the assertion. ∎

We are now ready to bound $\| u - u^c_{hp} \|_{\mathrm{E},\mathcal{T}}$ in (4.6).

LEMMA 4.6. *Under the foregoing assumptions, the following upper bound holds*

$$\| u - u^c_{hp} \|_{\mathrm{E},\mathcal{T}} \lesssim \eta + \Theta.$$

Proof. Since $u - u^c_{hp} \in H^1_0(\Omega)$, we have that

$$\| u - u^c_{hp} \|_{\mathrm{E},\mathcal{T}} = \frac{A(u - u^c_{hp}, v)}{\| v \|_{\mathrm{E},\mathcal{T}}}, \tag{4.10}$$

where $v = u - u_{hp}$. To bound the right-hand side of (4.10), we note that, by (1.2) and property (4.7),

$$A(u - u^c_{hp}, v) = \int_\Omega fv\,dx - A(u^c_{hp}, v) = \int_\Omega fv\,dx - D_{hp}(u^c_{hp}, v).$$

One can now readily see that

$$D_{hp}(u^c_{hp}, v) = D_{hp}(u_{hp}, v) + R,$$

with

$$R = -\sum_{\widetilde{K}\in\widetilde{\mathcal{T}}} \int_{\widetilde{K}} \nabla u^r_{hp} \cdot \nabla v\,dx.$$

Here, we have also used that the jumps of v vanish. Furthermore, from the DG method in (2.6) and property (4.8), we have

$$\int_\Omega fv_{hp}\,dx = D_{hp}(u_{hp}, v_{hp}) + K_{hp}(u_{hp}, v_{hp}),$$

where $v_{hp} \in S_{\underline{p}}(\mathcal{T})$ is the hp-version approximation of v in (4.9). Combining these results, we thus arrive at

$$A(u - u^c_{hp}, v) = \int_\Omega f(v - v_{hp})\,dx - D_{hp}(u_{hp}, v - v_{hp}) + K_{hp}(u_{hp}, v_{hp}) - R,$$

The estimate in Lemma 4.5 now yields

$$|A(u - u^c_{hp}, v)| \lesssim (\eta + \Theta)\,|\!|\!|\, v \,|\!|\!|_{\mathrm{E},\mathcal{T}} + |R|. \tag{4.11}$$

It remains to bound $|R|$; from the Cauchy-Schwarz inequality and Lemma 4.4, we readily obtain

$$|R| \lesssim |\!|\!|\, u^r_{hp} \,|\!|\!|_{\mathrm{E},\widetilde{\mathcal{T}}}\, |\!|\!|\, v \,|\!|\!|_{\mathrm{E},\mathcal{T}} \lesssim \eta\, |\!|\!|\, v \,|\!|\!|_{\mathrm{E},\mathcal{T}}. \tag{4.12}$$

The desired result now follows from (4.10), (4.11) and (4.12). ∎

The proof of Theorem 3.1 readily follows from (4.6), Lemma 4.4 and Lemma 4.6.

5. Proof of Theorem 4.1. In this section, we prove the result of Theorem 4.1.

5.1. Polynomial basis functions. As in the proof of [32, Theorem 4.5], we begin by introducing polynomial basis functions. To that end, let $\widehat{I} = (-1, 1)$ be the reference interval. We denote by $\widehat{\mathcal{Z}}^p(\widehat{I}) = \{\, \widehat{z}^p_0, \cdots, \widehat{z}^p_p \,\}$ the Gauss-Lobatto nodes of order $p \geq 1$ on $\widehat{I}$. Recall that $\widehat{z}^p_0 = -1$ and $\widehat{z}^p_p = 1$. We denote by $\widehat{\mathcal{Z}}^p_{\mathrm{int}}(\widehat{I}) = \{\, \widehat{z}^p_1, \cdots, \widehat{z}^p_{p-1} \,\}$ the interior Gauss-Lobatto nodes of order p on $\widehat{I}$.

Now let $E \in \mathcal{E}(K)$ be an elemental edge of $K \in \mathcal{T}$. The nodes in $\widehat{\mathcal{Z}}^p$ can be affinely mapped onto E and we denote by $\mathcal{Z}^p(E) = \{\, z^{E,p}_0, \cdots, z^{E,p}_p \,\}$ the Gauss-Lobatto nodes of order p on E. The points $z^{E,p}_0$ and $z^{E,p}_p$ coincide with the two end points of E. The set $\mathcal{Z}^p_{\mathrm{int}}(E) = \{\, z^{E,p}_1, \cdots, z^{E,p}_{p-1} \,\}$ denotes the interior Gauss-Lobatto points of order p. We write $\mathcal{P}_p(E)$ for the space of all polynomials of degree less than or equal to p on E and define

$$\mathcal{P}^{\mathrm{int}}_p(E) = \{\, q \in \mathcal{P}_p(E) \;:\; q(z^{E,p}_0) = q(z^{E,p}_p) = 0 \,\},$$
$$\mathcal{P}^{\mathrm{nod}}_p(E) = \{\, q \in \mathcal{P}_p(E) \;:\; q(z) = 0,\ z \in \mathcal{Z}^p_{\mathrm{int}}(E) \,\}.$$

By construction, we have $\mathcal{P}_p(E) = \mathcal{P}_p^{\rm int}(E) \oplus \mathcal{P}_p^{\rm nod}(E)$.

On the reference square $\widehat{I}^2 = (-1,1)^2$, we define the tensor-product Gauss-Lobatto nodes of order p by $\widehat{\mathcal{Z}}^p(\widehat{I}^2) = \{\, \widehat{z}^p_{i,j} = (\widehat{z}^p_i, \widehat{z}^p_j) \,\}_{0\le i,j\le p}$. These nodes can be affinely mapped onto an elemental face $F \in \mathcal{F}(K)$ of $K \in \mathcal{T}$ and we define $\mathcal{Z}^p(F) = \{\, z^{F,p}_{i,j} \,\}_{0\le i,j\le p}$ to be the Gauss-Lobatto nodes of order p on F. Furthermore, we write $\mathcal{Z}^p_{\rm int}(F) = \{\, z^{F,p}_{i,j} \,\}_{1\le i,j\le p-1}$ for the interior Gauss-Lobatto points on F. We also define

$$\mathcal{Q}^{\rm int}_{p_F}(F) = \{\, q \in \mathcal{Q}_{p_F}(F) \;:\; q = 0 \text{ on } \partial F\}.$$

Similarly, we define the interior Gauss-Lobatto nodes of order p on the reference element $\widehat{K}$ by $\widehat{\mathcal{Z}}^p_{\rm int}(\widehat{K}) = \{\widehat{z}^p_{i,j,k} = (\widehat{z}^p_i, \widehat{z}^p_j, \widehat{z}^p_k)\}_{1\le i,j,k\le p-1}$. For an element $K \in \mathcal{T}$ and a polynomial degree $p \ge 1$, we denote its interior Gauss-Lobatto points by $\mathcal{Z}^p_{\rm int}(K) = \{\, z^{K,p}_{i,j,k} \,\}_{1\le i,j,k\le p-1}$. Here, the points $z^{K,p}_{i,j,k}$ are the affine mappings of $\widehat{z}^p_{i,j,k}$ onto the element K.

Suppose now that we are given edge and face polynomial degrees $1 \le p_E \le p$ and $1 \le p_F \le p$, associated with the elemental edges $E \in \mathcal{E}(K)$ and elemental faces $F \in \mathcal{F}(K)$. We assume that $p_E \le p_F$ for $E \in \mathcal{E}(F)$. We shall define basis functions for polynomials $v \in \mathcal{Q}_p(K)$ with the restriction that

$$v|_E \in \mathcal{P}_{p_E}(E), \quad E \in \mathcal{E}(K), \qquad\qquad v|_F \in \mathcal{Q}_{p_F}(F), \quad F \in \mathcal{F}(K). \tag{5.1}$$

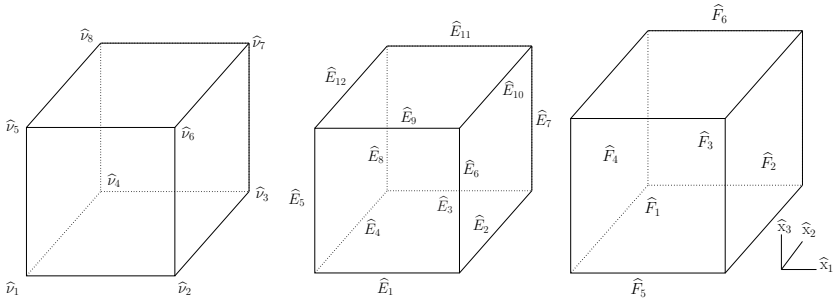

(a) Numbering of nodes (b) Numbering of edges (c) Numbering of faces

FIG. 5.1. *Reference element $\widehat{K}$ with the numbering of faces, edges and vertices.*

As usual, we shall divide the basis functions into interior, face, edge and vertex basis functions. We first consider the reference element $K = \widehat{K} = (-1,1)^3$. We denote its faces by $\widehat{F}_1, \ldots \widehat{F}_6$, its edges by $\widehat{E}_1, \ldots, \widehat{E}_{12}$ and its vertices by $\widehat{\nu}_1, \ldots, \widehat{\nu}_8$, numbered as in Figure 5.1. Let $\{\widehat{\varphi}^p_i\}_{0\le i\le p}$ be the Lagrange basis functions associated with the Gauss-Lobatto nodes $\widehat{\mathcal{Z}}^p(\widehat{I})$ on $\widehat{I}$. The interior basis functions are then

$$\widehat{\Phi}^{{\rm int},p}_{i,j,k}(\widehat{x}_1,\widehat{x}_2,\widehat{x}_3) = \widehat{\varphi}^p_i(\widehat{x}_1)\,\widehat{\varphi}^p_j(\widehat{x}_2)\,\widehat{\varphi}^p_k(\widehat{x}_3), \qquad 1 \le i,j,k \le p-1.$$

Next, we define the face basis functions exemplary for the face $\widehat{F}_1$ in Figure 5.1 with face polynomial degree $p_{\widehat{F}_1}$. They are given by

$$\widehat{\Phi}^{\widehat{F}_1,p_{\widehat{F}_1}}_{i,j}(\widehat{x}_1,\widehat{x}_2,\widehat{x}_3) = \widehat{\varphi}^{p_{\widehat{F}_1}}_i(\widehat{x}_1)\,\widehat{\varphi}^p_0(\widehat{x}_2)\,\widehat{\varphi}^{p_{\widehat{F}_1}}_j(\widehat{x}_3), \qquad 1 \le i,j \le p_{\widehat{F}_1} - 1.$$

Note that $\widehat{\Phi}_{i,j}^{\widehat{F}_1,p_{\widehat{F}_1}}$ vanishes on $\widehat{F}_2$ through $\widehat{F}_6$. The other face basis functions are then defined analogously. To define the edge basis functions, we consider exemplary the edge $\widehat{E}_1$ in Figure 5.1 with edge degree $p_{\widehat{E}_1}$. The edge basis functions for $\widehat{E}_1$ are

$$\widehat{\Phi}_i^{\widehat{E}_1,p_{\widehat{E}_1}}(\widehat{x}_1,\widehat{x}_2,\widehat{x}_3) = \widehat{\varphi}_i^{p_{\widehat{E}_1}}(\widehat{x}_1)\,\widehat{\varphi}_0^{p_{\widehat{F}_5}}(\widehat{x}_2)\,\widehat{\varphi}_0^{p_{\widehat{F}_1}}(\widehat{x}_3), \qquad i=1,\dots,p_{\widehat{E}_1}-1.$$

Note that $\widehat{\Phi}_i^{\widehat{E}_1,p_{\widehat{E}_1}}$ vanishes on all the other edges and on the faces $\widehat{F}_2$, $\widehat{F}_3$, $\widehat{F}_4$ and $\widehat{F}_6$. Moreover, it vanishes on the interior nodes $\{\widehat{z}_{i,j}^{\widehat{F}_1,p_{\widehat{F}_1}}\}_{i,j=1}^{p_{\widehat{F}_1}-1}$ and $\{\widehat{z}_{i,j}^{\widehat{F}_5,p_{\widehat{F}_5}}\}_{i,j=1}^{p_{\widehat{F}_5}-1}$ of the faces $\widehat{F}_1$ and $\widehat{F}_5$, respectively. The other edge basis functions are then defined analogously. Finally, we consider the vertex $\widehat{\nu}_1$, which is shared by the edges $\widehat{E}_1$, $\widehat{E}_4$ and $\widehat{E}_5$; see Figure 5.1. The associated vertex basis function is then defined by

$$\widehat{\Phi}_{\widehat{K}}^{\widehat{\nu}_1}(\widehat{x}_1,\widehat{x}_2,\widehat{x}_3) = \widehat{\varphi}_0^{p_{\widehat{E}_1}}(\widehat{x}_1)\,\widehat{\varphi}_0^{p_{\widehat{E}_4}}(\widehat{x}_2)\,\widehat{\varphi}_0^{p_{\widehat{E}_5}}(\widehat{x}_3).$$

The vertex basis functions associated with the other vertices of $\widehat{K}$ can be defined analogously. This completes the definition of the shape functions on the reference element $\widehat{K}$.

For an arbitrary element K, the basis functions Φ on K can be defined from the analogous ones on $\widehat{K}$ by the pull-back map T_K: $\Phi(x_1,x_2,x_3) = \widehat{\Phi}\circ T_K^{-1}(x_1,x_2,x_3)$, giving rise to shape functions Φ_K^ν, Φ_i^{E,p_E}, $\Phi_{i,j}^{F,p_F}$ and $\Phi_{i,j,k}^{\mathrm{int},p}$ on K. Therefore, a polynomial $v\in\mathcal{Q}_p(K)$ satisfying (5.1) can be expanded in the following form:

$$\begin{aligned} v(x) = &\sum_{\nu\in\mathcal{N}(K)} v(\nu)\,\Phi_K^\nu(x) + \sum_{E\in\mathcal{E}(K)}\sum_{i=1}^{p_E-1} v(z_i^{E,p_E})\,\Phi_i^{E,p_E}(x) \\ &+ \sum_{F\in\mathcal{F}(K)}\sum_{i,j=1}^{p_F-1} c_{i,j}^F \Phi_{i,j}^{F,p_F}(x) + \sum_{1\le i,j,k\le p-1} c_{i,j,k}\,\Phi_{i,j,k}^{\mathrm{int},p}(x), \end{aligned}$$

with coefficients $c_{i,j}^F$ and $c_{i,j,k}$.

In the sequel, we will make use of the following two estimates for polynomials, which are proven in Lemma 3.1 of [9]; see also [32].

LEMMA 5.1. *For an element K, we have the following estimates:*

(i) If $v\in\mathcal{Q}_{p_K}(K)$ vanishes at the interior tensor-product Gauss-Lobatto nodes of K, then there holds

$$\|v\|_{L^2(K)}^2 \lesssim h_K p_K^{-2}\|v\|_{L^2(\partial K)}^2.$$

(ii) If the vertex ν of K is shared by the elemental edges E_i, E_j and E_k, then the vertex basis function Φ_K^ν can be bounded by

$$\|\Phi_K^\nu\|_{L^2(K)} \lesssim h_K^{3/2} p_{E_i}^{-1} p_{E_j}^{-1} p_{E_k}^{-1}.$$

(iii) Let the elemental face F be spanned by the two elemental edges E_i and E_j. Suppose that the vertex ν is given by the intersection of E_i and E_j. Then the vertex basis Φ_K^ν can be bounded by

$$\|\Phi_K^\nu\|_{L^2(F)} \lesssim h_K p_{E_i}^{-1} p_{E_j}^{-1}.$$

5.2. Edge extension operators. In this section, we define extension operators over an edge E. To that end, fix an element $K \in \mathcal{T}$. We discuss three cases where we shall employ edge extensions. First, if $E \in \mathcal{E}(K)$ is an elemental edge of K without a hanging node, we define the edge extension operator L_p^E by

$$L_{p,K}^E : \mathcal{P}_p^{\text{int}}(E) \longrightarrow \mathcal{Q}_p(K), \qquad q(x) \longmapsto \sum_{i=1}^{p-1} q(z_i^{E,p}) \Phi_i^{E,p}(x). \tag{5.2}$$

Second, if the edge $E \in \mathcal{E}(K)$ contains a hanging node located in the middle of E, then $E = E_1 \cup E_2$ for two mesh edges E_1 and E_2 in $\mathcal{E}(\mathcal{T})$. In this case, we partition K into two parallelepipeds, $K = K_1 \cup K_2$, by connecting the hanging node on E with the midpoint of the edge parallel to E, as illustrated in Figure 5.2. For $q_1 \in \mathcal{P}_p^{\text{int}}(E_1)$ and $q_2 \in \mathcal{P}_p^{\text{int}}(E_2)$, we then define the extension operator $L_{p,K}^E(q_1, q_2)$ by

$$L_{p,K}^E(q_1, q_2) = L_{p,K_1}^{E_1}(q_1) + L_{p,K_2}^{E_2}(q_2), \tag{5.3}$$

with $L_{p,K_1}^{E_1}(\cdot)$ and $L_{p,K_2}^{E_2}(\cdot)$ given in (5.2).

The third case arises if the edge E belongs to the space

$$\mathcal{E}_F(K) = \{\, E \in \mathcal{E}(\mathcal{T}) \;:\; E \text{ is inside } F \,\} \tag{5.4}$$

for an elemental face $F \in \mathcal{F}(K)$. That is, $E \in \mathcal{E}_F(K)$ is one of the four mesh edges whose intersection is a hanging node located in the middle of F. This situation is depicted in Figure 5.3. In this case, we partition $K = \cup_{i=1}^4 K_i$ into four elements, as illustrated in Figure 5.3. If E is shared by K_1 and K_2 and if $q \in \mathcal{P}_p^{\text{int}}(E)$, the extension $L_{p,K}^E(q)$ is then defined by

$$L_{p,K}^E(q) = L_{p,K_1}^E(q) + L_{p,K_2}^E(q), \tag{5.5}$$

with L_{p,K_1}^E and L_{p,K_2}^E given in (5.2) and extended by zero to the other two elements.

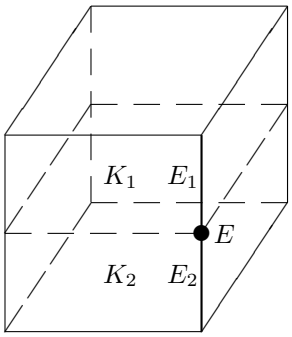

FIG. 5.2. *Case 2: The elemental edge $E \in \mathcal{E}(K)$ has a hanging node located in its midpoint.*

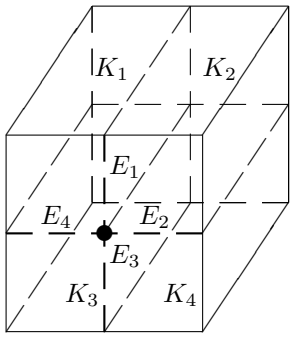

FIG. 5.3. *Case 3: The mesh edges E_i belong to $\mathcal{E}_F(K)$ for the elemental face F. The element K is then divided into four elements.*

By construction, the extension operators $L_{p,K}^E(q)$ in (5.2), (5.5) and $L_{p,K}^E(q_1, q_2)$ in (5.3) are continuous on K and satisfy

$$L_{p,K}^E(q)|_E = q, \qquad L_{p,K}^E(q_1, q_2)|_{E_1} = q_1, \qquad L_{p,K}^E(q_1, q_2)|_{E_2} = q_2.$$

Moreover, $L^E_{p,K}(q)$ and $L^E_{p,K}(q_1,q_2)$ both vanish at the interior Gauss-Lobatto nodes in $\mathcal{Z}^p_{\rm int}(K)$, on the other edges of $\mathcal{E}(K)$ and the elemental faces in $\mathcal{F}(K)$ not containing E. From [9, Lemma 3.1], we have the following inequalities.

LEMMA 5.2. *The linear edge extension operators L^E_p introduced above satisfy*

$$\begin{aligned}
\|L^E_{p,K}(q)\|_{L^2(K)} &\lesssim p^{-2}h_K\|q\|_{L^2(E)}, && E\in\mathcal{E}(K),\\
\|L^E_{p,K}(q)\|_{L^2(K)} &\lesssim p^{-2}h_K\|q\|_{L^2(E)}, && E\in\mathcal{E}_F(K),\ F\in\mathcal{F}(K),\\
\|L^E_{p,K}(q_1,q_2)\|_{L^2(K)} &\lesssim p^{-2}h_K\sum_{i=1}^2\|q_i\|_{L^2(E_i)}, && E\in E_1\cup E_2,\ E_1,E_2\in\mathcal{E}(\mathcal{T}).
\end{aligned}$$

5.3. Face extension operators. Next, we define extension operators over faces. To that end, fix an element $K\in\mathcal{T}$ and let $F\in\mathcal{F}(K)$ be an elemental face of K. Again, we shall discuss three cases of face extensions. First, if there is no hanging node of $\mathcal{T}$ located on F (i.e., $F\in\mathcal{F}(\mathcal{T})\cap\mathcal{F}(\widetilde{\mathcal{T}})$ or $F\in\mathcal{F}_N(\mathcal{T})$), we define $L^F_{p,K}$ by

$$L^F_{p,K}:\mathcal{Q}^{\rm int}_p(F)\longrightarrow\mathcal{Q}_p(K),\qquad q(x)\longmapsto\sum_{i,j=1}^{p-1}q(z^{F,p}_{i,j})\Phi^{F,p}_{i,j}(x). \tag{5.6}$$

Second, if F has a hanging node in its midpoint (i.e., $F\notin\mathcal{F}(\mathcal{T})$), we write F as $F=\cup_{i=1}^4F_i$, for four faces $F_i\in\mathcal{F}(\mathcal{T})$. We then partition K into four parallelepipeds, $K=\cup_{i=1}^4K_i$, as illustrated in Figure 5.4. For polynomials $q_i\in\mathcal{Q}^{\rm int}_p(F_i)$, $i=1,\ldots,4$, we define the operator $L^F_{p,K}(q_1,q_2,q_3,q_4)$ by

$$L^F_{p,K}(q_1,q_2,q_3,q_4)=\sum_{i=1}^4L^{F_i}_{p,K_i}(q_i), \tag{5.7}$$

with $L^{E_i}_{p,K_i}$, $i=1,\ldots,4$, given in (5.6).

Third, if F contains a hanging node located on one of its elemental edges (i.e., $F\in\mathcal{F}_H(\mathcal{T})$), we divide F into four faces $F_1,\ldots,F_4\in\mathcal{F}(\widetilde{\mathcal{T}})$ and again partition K into four parallelepipeds, $K=\cup_{i=1}^4K_i$, as shown in Figure 5.5. We denote by ν_c the center of F. If $q\in\mathcal{Q}_p(F)$ with $q=0$ on ∂F, we define the extension operator $L^F_{p,K}(q)$ by

$$L^F_{p,K}(q)=\sum_{i=1}^4L^{F_i}_{p,K_i}(q|_{F_i}), \tag{5.8}$$

where, for $1\le i\le 4$,

$$L^{F_i}_{p,K_i}(q|_{F_i})=\sum_{k,l=1}^{p-1}q(z^{F_i,p}_{k,l})\Phi^{F_i,p}_{k,l}+\sum_{E\in\mathcal{E}(F_i)}\sum_{k=1}^{p-1}q(z^{E,p}_k)\Phi^{E,p}_k+q(\nu_c)\Phi^{\nu_c}_{K_i}.$$

By definition, the face extensions $L^F_{p,K}(q)$ in (5.7), (5.8) and $L^F_{p,K}(q_1,q_2,q_3,q_4)$ in (5.7) are continuous on K and satisfy

$$L^F_{p,K}(q)|_F=q,\qquad L^F_{p,K}(q_1,q_2,q_3,q_4)|_{E_i}=q_i,\qquad i=1,\ldots,4.$$

Moreover, $L^F_{p,K}(q)$ and $L^F_{p,K}(q_1,q_2,q_3,q_4)$ both vanish in the interior Gauss-Lobatto nodes in $\mathcal{Z}^p_{\rm int}(K)$ and on the elemental faces of K not equal to F. From [9, Lemma 3.1], we have the following inequalities.

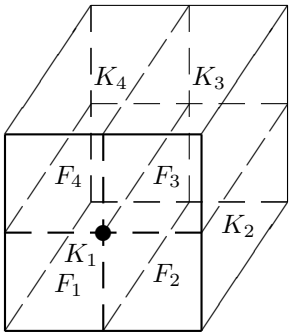

FIG. 5.4. *Case 2: Partition of K associated with the partition of face F.*

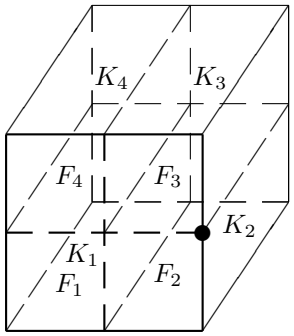

FIG. 5.5. *Case 3: Partition of K associated with the partition of face F.*

LEMMA 5.3. *The linear face extension operators $L^F_{p,K}$ introduced above satisfy*

$$\|L^F_{p,K}(q)\|_{L^2(K)} \lesssim p^{-1}h_K^{1/2}\|q\|_{L^2(F)}, \qquad F \in \mathcal{F}(\mathcal{T}) \cap \mathcal{F}(\widetilde{\mathcal{T}}) \text{ or } F \in \mathcal{F}_N(\mathcal{T}),$$

$$\|L^F_{p,K}(q)\|_{L^2(K)} \lesssim p^{-1}h_K^{1/2}\|q\|_{L^2(F)}, \qquad F \in \mathcal{F}_H(\mathcal{T}),$$

$$\|L^F_{p,K}(q_1,\dots,q_4)\|_{L^2(K)} \lesssim p^{-1}h_K^{1/2}\sum_{i=1}^4 \|q_i\|_{L^2(F_i)},\ F = \cup_{i=1}^4 F_i,\ F_1,\dots,F_4 \in \mathcal{F}(\mathcal{T}).$$

5.4. Decomposition of functions in $S_{\underline{p}}(\mathcal{T})$. We shall now decompose functions in $S_{\underline{p}}(\mathcal{T})$, in a similar manner to the construction in [32, Section 5.3]. To this end, we first define the minimal edge and face degrees. For an edge $E \in \mathcal{E}(\mathcal{T}) \cup \mathcal{E}(\widetilde{\mathcal{T}})$ and a face $F \in \mathcal{F}(\mathcal{T}) \cup \mathcal{F}(\widetilde{\mathcal{T}})$, we set

$$\begin{aligned} \overline{p}_E &= \min\{\, p_{\widetilde{K}} \,:\, \widetilde{K} \in \mathcal{T} \cup \widetilde{\mathcal{T}},\ E \in \mathcal{E}(\widetilde{K})\,\}, \\ \overline{p}_F &= \min\{\, p_{\widetilde{K}} \,:\, \widetilde{K} \in \mathcal{T} \cup \widetilde{\mathcal{T}},\ F \in \mathcal{F}(\widetilde{K})\,\}. \end{aligned} \tag{5.9}$$

Let $v \in S_{\underline{p}}(\mathcal{T})$. We denote by v_K the restriction of v to an element $K \in \mathcal{T} \cup \widetilde{\mathcal{T}}$. We decompose v into a nodal, edge, face and interior part, respectively:

$$v = v^{\mathrm{nod}} + v^{\mathrm{edge}} + v^{\mathrm{face}} + v^{\mathrm{int}}, \tag{5.10}$$

with v^{nod}, v^{edge}, v^{face} and v^{int} in $S_{\underline{\widetilde{p}}}(\widetilde{\mathcal{T}})$ introduced below.

5.4.1. Nodal part. First, we construct the nodal part $v^{\mathrm{nod}} \in S_{\underline{\widetilde{p}}}(\widetilde{\mathcal{T}})$ in (5.10). For each element $K \in \mathcal{T}$ and $\widetilde{K} \in \mathcal{R}(K)$, we will construct the restriction $v^{\mathrm{nod}}_{\widetilde{K}}$ of v^{nod} to $\widetilde{K}$ such that $v^{\mathrm{nod}}_{\widetilde{K}} \in \mathcal{Q}_{p_{\widetilde{K}}}(\widetilde{K})$ (note that $p_K = p_{\widetilde{K}}$) and

$$v^{\mathrm{nod}}_{\widetilde{K}}|_E \in \mathcal{P}_{\overline{p}_E}(E), \quad E \in \mathcal{E}(\widetilde{K}), \qquad v^{\mathrm{nod}}_{\widetilde{K}}|_F \in \mathcal{P}_{\overline{p}_F}(F), \quad F \in \mathcal{F}(\widetilde{K}),$$

with $\overline{p}_E$ and $\overline{p}_F$ given in (5.9). To define $v^{\mathrm{nod}}_{\widetilde{K}}$, we distinguish the following two cases.

Case 1: If $\mathcal{R}(K) = \{K\}$ (i.e., if K is unrefined), the interpolant $v^{\mathrm{nod}}_{\widetilde{K}} = v^{\mathrm{nod}}_K$ is simply defined by

$$v^{\mathrm{nod}}_K(x) = \sum_{\nu \in \mathcal{N}(K)} v_K(\nu)\ \Phi^\nu_K(x). \tag{5.11}$$

Case 2: If $\mathcal{R}(K)$ consists of eight newly created elements, we define $v_{\widetilde{K}}^{\mathrm{nod}}$ on each element $\widetilde{K} \in \mathcal{R}(K)$ separately. To do so, fix $\widetilde{K} \in \mathcal{R}(K)$. Without loss of generality, we may consider the situation shown in Figure 5.6, where we denote by $\widetilde{\nu}_i$, $\widetilde{E}_j$ and $\widetilde{F}_k$ the vertices, edges and faces of $\widetilde{K}$, respectively, numbered as in Figure 5.1. Similarly, we denote by ν_i, E_j and F_k the vertices, edges and faces of K, respectively.

In this configuration, notice that we have $\widetilde{\nu}_8 \in \mathcal{N}_A(\widetilde{\mathcal{T}})$, $\widetilde{F}_3, \widetilde{F}_4, \widetilde{F}_6 \in \mathcal{F}_A(\widetilde{\mathcal{T}})$, as well as $\widetilde{E}_8, \widetilde{E}_{11}, \widetilde{E}_{12} \in \mathcal{E}_A(\widetilde{\mathcal{T}})$. Hence, the polynomial degrees are given by

$$\overline{p}_{\widetilde{F}_i} = \overline{p}_{\widetilde{E}_j} = p_{\widetilde{K}} = p_K, \qquad i \in \{3,4,6\},\ j \in \{8,11,12\}.$$

Let us now define the value of $v_{\widetilde{K}}^{\mathrm{nod}}$ at the nodes located on $\partial\widetilde{K}$. At the interior nodes shared by $\widetilde{F}_i$ and $\widetilde{E}_j$ for $i \in \{3,4,6\}$ and $j \in \{8,11,12\}$, we set

$$v_{\widetilde{K}}^{\mathrm{nod}}(z) = v_K(z), \qquad z \in \{\mathcal{Z}_{\mathrm{int}}^{p_{\widetilde{F}_i}}(\widetilde{F}_i)\}_{i\in\{3,4,6\}} \cup \{\mathcal{Z}_{\mathrm{int}}^{p_{\widetilde{E}_j}}(\widetilde{E}_j)\}_{j\in\{8,11,12\}}. \tag{5.12}$$

Similarly, we set $v_{\widetilde{K}}^{\mathrm{nod}}(\nu) = v_K(\nu)$ for the vertices $\nu = \widetilde{\nu}_2$ and $\nu = \widetilde{\nu}_8$.

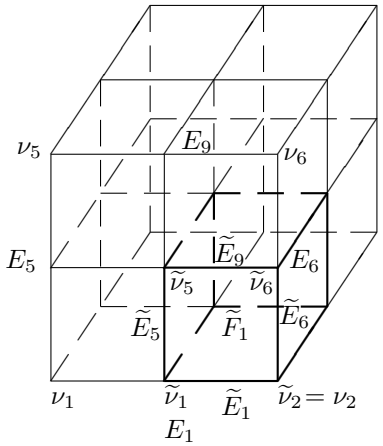

FIG. 5.6. *The element K is refined into* 8 *elements $\widetilde{K} \in \mathcal{R}(K)$.*

It remains to define $v_{\widetilde{K}}^{\mathrm{nod}}$ on the nodes located on the faces $\widetilde{F}_1$, $\widetilde{F}_2$ and $\widetilde{F}_5$ (excluding the vertex $\widetilde{\nu}_2$). We only consider $\widetilde{F}_1$ (the construction for $\widetilde{F}_2$ and $\widetilde{F}_5$ is completely analogous); see Figure 5.6. If $\widetilde{F}_1 \in \mathcal{F}(\mathcal{T})$, then we have $\widetilde{\nu}_1, \widetilde{\nu}_5, \widetilde{\nu}_6 \in \mathcal{N}(\mathcal{T})$. The four edges $\widetilde{E}_i \in \mathcal{E}(\widetilde{F}_1)$ for $i \in \{1,5,6,9\}$ belong to $\mathcal{E}(\mathcal{T})$. For $i \in \{1,5,6,9\}$ and $j \in \{1,5,6\}$, we define

$$v_{\widetilde{K}}^{\mathrm{nod}}(z) = 0, \qquad z \in \mathcal{Z}_{\mathrm{int}}^{\overline{p}_{\widetilde{F}_1}}(\widetilde{F}_1) \cup \{\mathcal{Z}_{\mathrm{int}}^{\overline{p}_{\widetilde{E}_i}}(\widetilde{E}_i)\}_{\widetilde{E}_i \in \mathcal{E}(\widetilde{F}_1)}, \tag{5.13}$$

$$v_{\widetilde{K}}^{\mathrm{nod}}(\widetilde{\nu}_j) = v_K(\widetilde{\nu}_j). \tag{5.14}$$

Otherwise, if $\widetilde{F}_1 \notin \mathcal{F}(\mathcal{T})$, then the large elemental face F_1 belongs to $\mathcal{F}_R(\mathcal{T})$. Moreover, we have that either $F_1 \in \mathcal{F}_N(\mathcal{T})$ or $F_1 \in \mathcal{F}_H(\mathcal{T})$. We distinguish these two subcases. First, if $F_1 \in \mathcal{F}_N(\mathcal{T})$, then there is no hanging node of $\mathcal{T}$ located on F_1 or any edge of F_1, and we have $\overline{p}_{\widetilde{F}_1} = \overline{p}_{F_1}$. In this case, we interpolate the values of the nodal interpolant over the face F_1 at the Gauss-Lobatto nodes on $\widetilde{F}_1$. That is, we

define

$$v_{\widetilde{K}}^{\mathrm{nod}}(z) = \sum_{\nu \in \mathcal{N}(F_1)} v_K(\nu)\, \Phi_K^{\nu}(z), \tag{5.15}$$

for all $z \in \{\mathcal{Z}_{\mathrm{int}}^{\overline{p}_{\widetilde{E}}}(\widetilde{E})\}_{\widetilde{E}\in\mathcal{E}(\widetilde{F}_1)} \cup \mathcal{Z}_{\mathrm{int}}^{\overline{p}_{\widetilde{F}_1}}(\widetilde{F}_1) \cup \{\widetilde{\nu}_i\}_{i\in\{1,5,6\}}$.

Second, if $F_1 \in \mathcal{F}_H(\mathcal{T})$, then $\widetilde{\nu}_5 \notin \mathcal{N}(\mathcal{T})$, but $\widetilde{\nu}_1$ and $\widetilde{\nu}_6$ may or may not belong to $\mathcal{N}(\mathcal{T})$. We define the value of $v_{\widetilde{K}}^{\mathrm{nod}}$ at the nodes located on $\widetilde{F}_1$ for this case as follows. First, noticing that $\overline{p}_{\widetilde{E}_5} = \overline{p}_{\widetilde{E}_9} = \overline{p}_{\widetilde{F}_1} = \overline{p}_{F_1}$ and $\widetilde{\nu}_2 \in \mathcal{N}(\mathcal{T})$, we set

$$v_{\widetilde{K}}^{\mathrm{nod}}(z) = 0, \qquad z \in \mathcal{Z}_{\mathrm{int}}^{\overline{p}_{F_1}}(\widetilde{F}_1) \cup \mathcal{Z}_{\mathrm{int}}^{\overline{p}_{F_1}}(\widetilde{E}_5) \cup \mathcal{Z}_{\mathrm{int}}^{\overline{p}_{F_1}}(\widetilde{E}_9) \cup \{\widetilde{\nu}_5\}, \tag{5.16}$$

Next, we define the values of $v_{\widetilde{K}}^{\mathrm{nod}}$ on the nodes of the edges $\widetilde{E}_1$ and $\widetilde{E}_6$, as well as on the nodes $\widetilde{\nu}_1$ and $\widetilde{\nu}_6$. We only consider $\widetilde{\nu}_1$ and $\widetilde{E}_1$ (the construction for $\widetilde{\nu}_6$ and $\widetilde{E}_6$ is completely analogous). If $\widetilde{\nu}_1 \in \mathcal{N}(\mathcal{T})$ (i.e., $\widetilde{\nu}_1$ is a hanging node in $\mathcal{T}$), then we define

$$v_{\widetilde{K}}^{\mathrm{nod}}(z) = 0, \quad z \in \mathcal{Z}_{\mathrm{int}}^{\overline{p}_{\widetilde{E}_1}}(\widetilde{E}_1), \qquad v_{\widetilde{K}}^{\mathrm{nod}}(\widetilde{\nu}_1) = v_K(\widetilde{\nu}_1). \tag{5.17}$$

If $\widetilde{\nu}_1 \notin \mathcal{N}(\mathcal{T})$, then we have $E_1 \in \mathcal{E}(\mathcal{T})$ and $\nu_1 \in \mathcal{N}(\mathcal{T})$. In this case, $\overline{p}_{\widetilde{E}_1} = \overline{p}_{E_1}$, and we interpolate the values of the nodal interpolant over the long edge E_1 at the Gauss-Lobatto nodes on $\widetilde{E}_1$. That is, we set

$$v_{\widetilde{K}}^{\mathrm{nod}}(z) = v_K(\nu_1)\, \Phi_K^{\nu_1}(z) + v_K(\nu_2)\, \Phi_K^{\nu_2}(z), \qquad z \in \mathcal{Z}_{\mathrm{int}}^{\overline{p}_{\widetilde{E}_1}}(\widetilde{E}_1) \cup \{\widetilde{\nu}_1\}. \tag{5.18}$$

With the nodal values of $v_{\widetilde{K}}^{\mathrm{nod}}$ constructed in (5.12)-(5.18), we have

$$\begin{aligned} v_{\widetilde{K}}^{\mathrm{nod}}(x) = & \sum_{\nu\in\mathcal{N}(\widetilde{K})} v_{\widetilde{K}}^{\mathrm{nod}}(\nu)\ \Phi_{\widetilde{K}}^{\nu}(x) + \sum_{E\in\mathcal{E}(\widetilde{K})} \sum_{i=1}^{\overline{p}_E - 1} \Big(v_{\widetilde{K}}^{\mathrm{nod}}(z_i^{E,\overline{p}_E}) \Phi_i^{E,\overline{p}_E}(x) \Big) \\ & + \sum_{F\in\mathcal{F}(\widetilde{K})} \sum_{i,j=1}^{\overline{p}_F - 1} \Big(v_{\widetilde{K}}^{\mathrm{nod}}(z_{i,j}^{F,\overline{p}_F}) \Phi_{i,j}^{F,\overline{p}_F}(x) \Big). \end{aligned}$$

This finishes the construction of the interpolant v^{nod}. Notice that $v^{\mathrm{nod}} \in S_{\underline{\widetilde{p}}}(\widetilde{\mathcal{T}})$; it is continuous over faces $F \in \mathcal{F}_A(\widetilde{\mathcal{T}})$ and over edges inside faces $F \in \mathcal{F}(\mathcal{T})$. Moreover, it satisfies

$$v_K(\nu) - v_K^{\mathrm{nod}}(\nu) = 0, \qquad \nu \in \mathcal{N}(\mathcal{T}) \text{ located on } \partial K,$$

and

$$v_{\widetilde{K}}^{\mathrm{nod}}|_E \in \mathcal{P}_{\overline{p}_E}^{\mathrm{nod}}(E), \qquad E \in \mathcal{E}(\mathcal{T}),\ \widetilde{K} \in \widetilde{w}_E,$$

with $\widetilde{w}_E$ defined by

$$\widetilde{w}_E = \{\, \widetilde{K} \in \mathcal{T} \cup \widetilde{\mathcal{T}} \,:\, E \in \mathcal{E}(\widetilde{K}) \,\}, \qquad \forall E \in \mathcal{E}(\mathcal{T}).$$

5.4.2. Edge part. Second, we construct the edge function $v^{\mathrm{edge}} \in S_{\underline{\widetilde{p}}}(\widetilde{\mathcal{T}})$ in the decomposition (5.10). To do so, fix an element $K \in \mathcal{T}$. For an edge E on ∂K, we define v_K^E by

$$v_K^E = \begin{cases} L^E_{p_K,K}((v_K - v_K^{\mathrm{nod}})|_E), & E \in \mathcal{E}(K) \cap \mathcal{E}(\mathcal{T}), \\ L^E_{p_K,K}((v_K - v_K^{\mathrm{nod}})|_E), & E \in \mathcal{E}_F(K),\ F \in \mathcal{F}(K), \\ L^E_{p_K,K}((v_K - v_K^{\mathrm{nod}})|_{E_1}, (v_K - v_K^{\mathrm{nod}})|_{E_2}), & E = E_1 \cup E_2,\ E_1, E_2 \in \mathcal{E}(\mathcal{T}), \end{cases}$$

with $L^E_{p_K,K}(\cdot)$ defined for Case 1 in (5.2) or for Case 3 in (5.5), and $L^E_{p_K,K}(\cdot,\cdot)$ for Case 2 in (5.3), respectively. We then define v^{edge} on each element as:

$$v_K^{\mathrm{edge}}(x) = \sum_{E \in \mathcal{E}(K)} v_K^E(x) + \sum_{F \in \mathcal{F}(K)} \sum_{E \in \mathcal{E}_F(K)} v_K^E(x).$$

5.4.3. Face part. Third, we construct the face function $v^{\mathrm{face}} \in S_{\underline{\widetilde{p}}}(\widetilde{\mathcal{T}})$ in (5.10). Fix an element $K \in \mathcal{T}$ and let F be an elemental face in $\mathcal{F}(K)$. If $F \in \mathcal{F}(\mathcal{T})$, we define v_K^F by

$$v_K^F = \begin{cases} L^F_{p_K,K}((v_K - v_K^{\mathrm{nod}} - v_K^{\mathrm{edge}})|_F), & F \notin \mathcal{F}_H(\mathcal{T}), \\ L^F_{p_K,K}((v_K - v_K^{\mathrm{nod}} - v_K^{\mathrm{edge}})|_F), & F \in \mathcal{F}_H(\mathcal{T}), \end{cases}$$

with $L^F_{p_K,K}(\cdot)$ defined for Case 1 in (5.6) and for Case 3 in (5.8). Otherwise, there exists four faces $F_i \in \mathcal{F}(\mathcal{T})$, $i = 1, \ldots, 4$, such that $F = \cup_{i=1}^4 \{F_i\}$. We define v_K^F by

$$v_K^F = L^F_{p_K,K}((v_K - v_K^{\mathrm{nod}} - v_K^{\mathrm{edge}})|_{F_1}, \ldots, (v_K - v_K^{\mathrm{nod}} - v_K^{\mathrm{edge}})|_{F_4}),$$

with $L^F_{p_K,K}(\cdot,\cdot,\cdot,\cdot)$ defined for Case 2 in (5.7). We then define v^{face} elementwise as

$$v_K^{\mathrm{face}}(x) = \sum_{F \in \mathcal{F}(K)} v_K^F(x).$$

5.5. Interior part. Finally, the interior function $v^{\mathrm{int}} \in S_{\underline{\widetilde{p}}}(\widetilde{\mathcal{T}})$ in (5.10) is simply obtained by setting on each element

$$v_K^{\mathrm{int}} = v_K - v_K^{\mathrm{nod}} - v_K^{\mathrm{edge}} - v_K^{\mathrm{face}}, \qquad K \in \mathcal{T}.$$

Notice that v_K^{int} belongs to $H_0^1(K)$. Hence, we have $v^{\mathrm{int}} \in S^c_{\underline{\widetilde{p}}}(\widetilde{\mathcal{T}})$.

5.6. Proof of Theorem 4.1. In this section, we outline the proof of Theorem 4.1. Some of the auxiliary results are postponed to Sections 5.7.1, 5.7.2 and 5.7.3.

For $v \in S_{\underline{p}}(\mathcal{T})$, we write $v = v^{\mathrm{nod}} + v^{\mathrm{edge}} + v^{\mathrm{face}} + v^{\mathrm{int}}$, according to (5.10). We shall define the averaging operator $I_{hp}v$ in four parts:

$$I_{hp}v = \vartheta^{\mathrm{nod}} + \vartheta^{\mathrm{edge}} + \vartheta^{\mathrm{face}} + \vartheta^{\mathrm{int}}, \tag{5.19}$$

with ϑ^{nod}, $\vartheta^{\mathrm{edge}}$, $\vartheta^{\mathrm{face}}$, $\vartheta^{\mathrm{int}} \in S^c_{\underline{\widetilde{p}}}(\widetilde{\mathcal{T}})$. Since $v^{\mathrm{int}} \in S^c_{\underline{\widetilde{p}}}(\widetilde{\mathcal{T}})$, we simply take $\vartheta^{\mathrm{int}} = v^{\mathrm{int}}$. Below we further construct ϑ^{nod}, $\vartheta^{\mathrm{edge}}$, and $\vartheta^{\mathrm{face}}$ such that the following three approximation results hold.

PROPOSITION 5.4.

(i) Nodal approximation: *There is a conforming approximation* $\vartheta^{\mathrm{nod}} \in S^c_{\underline{p}}(\widetilde{\mathcal{T}})$ *that satisfies:*

$$\begin{aligned}\sum_{\widetilde{K}\in\widetilde{\mathcal{T}}} \|v^{\mathrm{nod}} - \vartheta^{\mathrm{nod}}\|^2_{L^2(\widetilde{K})} &\lesssim \sum_{F\in\mathcal{F}(\mathcal{T})} p_F^{-2} h_F \int_F [\![v^{\mathrm{nod}}]\!]^2 \, ds,\\ \sum_{\widetilde{K}\in\widetilde{\mathcal{T}}} \|\nabla(v^{\mathrm{nod}} - \vartheta^{\mathrm{nod}})\|^2_{L^2(\widetilde{K})} &\lesssim \sum_{F\in\mathcal{F}(\mathcal{T})} p_F^{2} h_F^{-1} \int_F [\![v^{\mathrm{nod}}]\!]^2 \, ds.\end{aligned} \tag{5.20}$$

(ii) Edge approximation: *There is a conforming approximation* $\vartheta^{\mathrm{edge}} \in S^c_{\underline{p}}(\widetilde{\mathcal{T}})$ *that satisfies:*

$$\begin{aligned}\sum_{\widetilde{K}\in\widetilde{\mathcal{T}}} \|v^{\mathrm{edge}} - \vartheta^{\mathrm{edge}}\|^2_{L^2(\widetilde{K})} &\lesssim \sum_{F\in\mathcal{F}(\mathcal{T})} p_F^{-2} h_F \int_F ([\![v]\!]^2 + [\![v^{\mathrm{nod}}]\!]^2) \, ds,\\ \sum_{\widetilde{K}\in\widetilde{\mathcal{T}}} \|\nabla(v^{\mathrm{edge}} - \vartheta^{\mathrm{edge}})\|^2_{L^2(\widetilde{K})} &\lesssim \sum_{F\in\mathcal{F}(\mathcal{T})} p_F^{2} h_F^{-1} \int_F ([\![v]\!]^2 + [\![v^{\mathrm{nod}}]\!]^2) \, ds.\end{aligned} \tag{5.21}$$

(iii) Face approximation: *There is a conforming approximation* $\vartheta^{\mathrm{face}} \in S^c_{\underline{p}}(\widetilde{\mathcal{T}})$ *that satisfies:*

$$\begin{aligned}\sum_{\widetilde{K}\in\widetilde{\mathcal{T}}} \|v^{\mathrm{face}} - \vartheta^{\mathrm{face}}\|^2_{L^2(\widetilde{K})} &\lesssim \sum_{F\in\mathcal{F}(\mathcal{T})} p_F^{-2} h_F \int_F ([\![v]\!]^2 + [\![v^{\mathrm{nod}}]\!]^2) \, ds,\\ \sum_{\widetilde{K}\in\widetilde{\mathcal{T}}} \|\nabla(v^{\mathrm{face}} - \vartheta^{\mathrm{face}})\|^2_{L^2(\widetilde{K})} &\lesssim \sum_{F\in\mathcal{F}(\mathcal{T})} p_F^{2} h_F^{-1} \int_F ([\![v]\!]^2 + [\![v^{\mathrm{nod}}]\!]^2) \, ds.\end{aligned} \tag{5.22}$$

By the triangle inequality and Proposition 5.4, we then obtain

$$\begin{aligned}\sum_{\widetilde{K}\in\widetilde{\mathcal{T}}} \|v - I_{hp} v\|^2_{L^2(\widetilde{K})} &\lesssim \sum_{F\in\mathcal{F}(\mathcal{T})} p_F^{-2} h_F (\|[\![v]\!]\|^2_{L^2(F)} + \|[\![v^{\mathrm{nod}}]\!]\|^2_{L^2(F)}),\\ \sum_{\widetilde{K}\in\widetilde{\mathcal{T}}} \|\nabla(v - I_{hp} v)\|^2_{L^2(\widetilde{K})} &\lesssim \sum_{F\in\mathcal{F}(\mathcal{T})} p_F^{2} h_F^{-1} (\|[\![v]\!]\|^2_{L^2(F)} + \|[\![v^{\mathrm{nod}}]\!]\|^2_{L^2(F)}).\end{aligned}$$

Hence, Theorem 4.1 follows if we show that

$$\|[\![v^{\mathrm{nod}}]\!]\|^2_{L^2(F)} \lesssim \|[\![v]\!]\|^2_{L^2(F)}, \qquad F \in \mathcal{F}(\mathcal{T}). \tag{5.23}$$

To prove (5.23), we define the set

$$\mathcal{N}_{\mathcal{T}}(F) = \{\, \nu \in \mathcal{N}(\mathcal{T}) \ : \ \nu \text{ is located on } \partial F \,\}, \qquad F \in \mathcal{F}(\mathcal{T}).$$

By the construction of v^{nod}, the jump over F satisfies

$$[\![v^{\mathrm{nod}}]\!](\nu) = [\![v]\!](\nu), \qquad \nu \in \mathcal{N}_{\mathcal{T}}(F).$$

If $F \in \mathcal{F}(\mathcal{T}) \cap \mathcal{F}(\widetilde{\mathcal{T}})$ or $F \in \mathcal{F}_N(\mathcal{T})$, then we have $\mathcal{N}(F) = \mathcal{N}_{\mathcal{T}}(F)$. Lemma 5.1(iii) and the bounded local variation of $\underline{p}$ in (2.3) yield

$$\|[\![v^{\mathrm{nod}}]\!]\|_{L^2(F)} \lesssim \sum_{\nu\in\mathcal{N}(F)} |[\![v^{\mathrm{nod}}(\nu)]\!]| \|\Phi^\nu_K\|_{L^2(F)} \lesssim \overline{p}_F^{-2} h_F \max_{\nu\in\mathcal{N}_{\mathcal{T}}(F)} |[\![v^{\mathrm{nod}}]\!](\nu)|,$$

with K one of the elements of which F is an elemental face.

Otherwise, we have $F \in \mathcal{F}_H(\mathcal{T})$. In this case, F is divided into four faces $\widetilde{F}_i \in \mathcal{F}(\widetilde{\mathcal{T}})$, $i = 1, \ldots, 4$, and the middle points of the elemental edges of F may or may not belong to $\mathcal{N}(\mathcal{T})$. This situation is the same as the one discussed for the two-dimensional case in [32, Section 5.5 (Case 2)]. Thus, proceeding as in the corresponding proof of Lemma 5.4 of [32], we obtain from (2.3) and the construction of v^{nod} that

$$\|[\![v^{\mathrm{nod}}]\!]\|_{L^2(F)} = \sum_{i=1}^{4} \|[\![v^{\mathrm{nod}}]\!]\|_{L^2(\widetilde{F}_i)} \lesssim \overline{p}_F^{-2} h_F \max_{\nu \in \mathcal{N}_{\mathcal{T}}(F)} |[\![v^{\mathrm{nod}}]\!](\nu)|.$$

Thus, for any face $F \in \mathcal{F}(\mathcal{T})$, we have

$$\|[\![v^{\mathrm{nod}}]\!]\|_{L^2(F)} \lesssim \overline{p}_F^{-2} h_F \max_{\nu \in \mathcal{N}_{\mathcal{T}}(F)} |[\![v^{\mathrm{nod}}]\!](\nu)| = \overline{p}_F^{-2} h_F \max_{\nu \in \mathcal{N}_{\mathcal{T}}(F)} |[\![v]\!](\nu)|.$$

Without loss of generality, we suppose that $|[\![v^{\mathrm{nod}}]\!](\nu)|$ reaches its maximum at the vertex ν_1, an end point of an edge $E \in \mathcal{E}(\mathcal{T})$ which lies on ∂F. From [29, Theorem 3.92], [9, Lemma 3.1] and (2.3), we further have the inverse estimate

$$\max_{\nu \in \mathcal{N}_{\mathcal{T}}(F)} \|[\![v]\!](\nu)\| = \|[\![v]\!](\nu_1)\| \lesssim p_E h_E^{-1/2} \|[\![v]\!]\|_{L^2(E)} \lesssim p_F^2 h_F^{-1} \|[\![v]\!]\|_{L^2(F)}.$$

This, together with the bounded local variation of $\underline{p}$ in (2.3), implies (5.23). To complete the proof of Theorem 4.1, it remains to prove Proposition 5.4, which will now be undertaken in the next section.

5.7. Proof of Proposition 5.4. In this section, we present the proofs of the three approximation results in Proposition 5.4.

5.7.1. Nodal approximation. Let $v^{\mathrm{nod}} \in S_{\underline{p}}(\widetilde{\mathcal{T}})$ be the nodal part of $v \in S_{\underline{p}}(\mathcal{T})$ in the decomposition (5.10). We shall now construct the conforming approximation ϑ^{nod} in $S^c_{\underline{p}}(\widetilde{\mathcal{T}})$. For simplicity, we shall omit the superscript "nod" and, in the sequel, write v for v^{nod} and ϑ for ϑ^{nod}. We introduce the sets:

$$\widetilde{w}(\nu) = \{\, \widetilde{K} \in \widetilde{\mathcal{T}} \,:\, \nu \in \mathcal{N}(\widetilde{K}) \,\}, \qquad w^F(\nu) = \{\, F \in \mathcal{F}(\mathcal{T}) \,:\, \nu \in F \,\}.$$

Fix $K \in \mathcal{T}$ and $\widetilde{K} \in \mathcal{R}(K)$. We proceed by distinguishing the same two cases as in Subsection 5.4.

Case 1: If $\mathcal{R}(K) = \{K\}$, we have $K = \widetilde{K}$. Then, any elemental face $\widetilde{F} \in \mathcal{F}(\widetilde{K})$ belongs to $\mathcal{F}(\mathcal{T})$ and we have $v_{\widetilde{K}}|_{\widetilde{F}} \in \mathcal{Q}_{\overline{p}_{\widetilde{F}}}(\widetilde{F})$. Moreover, any elemental edge $\widetilde{E} \in \mathcal{E}(\widetilde{K})$ belongs to $\mathcal{E}(\mathcal{T})$ and $v_{\widetilde{K}}|_{\widetilde{E}} \in \mathcal{P}^{\mathrm{nod}}_{\overline{p}_{\widetilde{E}}}(\widetilde{E})$. For any Gauss-Lobatto node ν located on $\partial\widetilde{K}$, we define the value of $\vartheta(\nu)$ by

$$\vartheta(\nu) = \begin{cases} |\widetilde{w}(\nu)|^{-1} \displaystyle\sum_{\widetilde{K} \in \widetilde{w}(\nu)} v_{\widetilde{K}}(\nu), & \nu \in \mathcal{N}_I(\mathcal{T}), \\ 0, & \text{otherwise.} \end{cases} \tag{5.24}$$

Here, $|\widetilde{w}(\nu)|$ denotes the cardinality of the set $\widetilde{w}(\nu)$. Note that we have $|\widetilde{w}(\nu)| = 8$ for $\nu \in \mathcal{N}_I(\mathcal{T})$. Then we define ϑ on $\widetilde{K}$ by:

$$\vartheta(x) = \sum_{\nu \in \mathcal{N}(\widetilde{K})} \vartheta(\nu)\, \Phi^{\nu}_{\widetilde{K}}(x). \tag{5.25}$$

¿From (5.11) and (5.25), we have

$$\|v_{\widetilde{K}} - \vartheta\|_{L^2(\widetilde{K})} \lesssim \sum_{\nu \in \mathcal{N}(\widetilde{K})} |v_{\widetilde{K}}(\nu) - \vartheta(\nu)| \, \|\Phi^{\nu}_{\widetilde{K}}\|_{L^2(\widetilde{K})}. \tag{5.26}$$

Analogously to [9, Pages 1125-1126], we conclude that

$$|v_{\widetilde{K}}(\nu) - \vartheta(\nu)| \lesssim \sum_{F \in w^F(\nu)} \overline{p}_F^2 h_F^{-1} \|[\![v]\!]\|_{L^2(F)}. \tag{5.27}$$

Hence, by combining (5.26), (5.27), Lemma 5.1(ii) and the bounded variation property of $\underline{p}$ in (2.3), we obtain

$$\|v_{\widetilde{K}} - \vartheta\|_{L^2(\widetilde{K})} \lesssim \sum_{F \in \{w^F(\nu)\}_{\nu \in \mathcal{N}(\widetilde{K})}} p_F^{-1} h_F^{1/2} \|[\![v]\!]\|_{L^2(F)}. \tag{5.28}$$

Case 2: If $\mathcal{R}(K)$ consists of eight elements, we define ϑ on each element $\widetilde{K} \in \mathcal{R}(K)$ separately, analogously to the construction of the nodal interpolant in Subsection 5.4. Without loss of generality, we may again consider the case illustrated in Figure 5.6. Since the faces $\widetilde{F}_3, \widetilde{F}_4, \widetilde{F}_6$ belong to $\mathcal{F}_A(\widetilde{\mathcal{T}})$, the function v is continuous over them. The values of ϑ on the face nodes $z \in \{\mathcal{Z}_{\rm int}^{p_{\widetilde{K}}}(\widetilde{F}_i)\}_{i\in\{3,4,6\}} \cup \{\mathcal{Z}_{\rm int}^{p_{\widetilde{K}}}(\widetilde{E}_j)\}_{j\in\{8,11,12\}}$ and the vertex $\widetilde{\nu}_8$ are defined by $\vartheta(\widetilde{\nu}_8) = v_{\widetilde{K}}(\widetilde{\nu}_8)$ and

$$\vartheta(z) = v_{\widetilde{K}}(z), \qquad z \in \{\mathcal{Z}_{\rm int}^{p_{\widetilde{K}}}(\widetilde{F}_i)\}_{i\in\{3,4,6\}} \cup \{\mathcal{Z}_{\rm int}^{p_{\widetilde{K}}}(\widetilde{E}_j)\}_{j\in\{8,11,12\}}. \tag{5.29}$$

We further define the value of ϑ on the vertex $\widetilde{\nu}_2$ by (5.24).

It remains to define the values of $v_{\widetilde{K}}$ on the nodes located on the faces $\widetilde{F}_1$, $\widetilde{F}_2$ and $\widetilde{F}_5$, excluding the vertex $\widetilde{\nu}_2$. We only consider $\widetilde{F}_1$ (the construction for $\widetilde{F}_2$ and $\widetilde{F}_5$ is completely analogous); see Figure 5.6. If $\widetilde{F}_1 \in \mathcal{F}(\mathcal{T})$, then for any Gauss-Lobatto node on $\widetilde{F}_1$, $z \in \mathcal{Z}_{\rm int}^{\overline{p}_{\widetilde{F}_1}}(\widetilde{F}_1) \cup \{Z_{\rm int}^{\overline{p}_E}(E)\}_{E\in\mathcal{E}(\widetilde{F}_1)} \cup \{\nu_1\} \cup \{\nu_5\} \cup \{\nu_6\}$, the value of $\vartheta(z)$ is taken as in (5.24).

Otherwise, if $\widetilde{F}_1 \notin \mathcal{F}(\mathcal{T})$, then $F_1 \in \mathcal{F}_R(\mathcal{T})$ and F_1 belongs to $\mathcal{F}_N(\mathcal{T})$ or $\mathcal{F}_H(\mathcal{T})$. We distinguish these two subcases. First, if $F_1 \in \mathcal{F}_N(\mathcal{T})$, we define $\vartheta(\nu)$, $\nu \in \mathcal{N}(F_1)$, by (5.24). Then we interpolate the values of the nodal interpolant over the face F_1 at the Gauss-Lobatto nodes on $\widetilde{F}_1$. That is, we set

$$\vartheta(z) = \sum_{\nu \in \mathcal{N}(F_1)} \vartheta(\nu) \, \Phi_K^{\nu}(z), z \in \{\mathcal{Z}_{\rm int}^{\overline{p}_{\widetilde{E}}}(\widetilde{E})\}_{\widetilde{E}\in\mathcal{E}(\widetilde{F}_1)} \cup \mathcal{Z}_{\rm int}^{\overline{p}_{\widetilde{F}_1}}(\widetilde{F}_1) \cup \{\widetilde{\nu}_i\}_{i\in\{1,5,6\}}. \tag{5.30}$$

Second, if $F_1 \in \mathcal{F}_H(\mathcal{T})$, then $\widetilde{\nu}_5 \notin \mathcal{N}(\mathcal{T})$, but $\widetilde{\nu}_1$ and $\widetilde{\nu}_6$ may or may not belong to $\mathcal{N}(\mathcal{T})$. We first define

$$\vartheta(z) = 0, \qquad z \in \mathcal{Z}_{\rm int}^{\overline{p}_{F_1}}(\widetilde{F}_1) \cup \mathcal{Z}_{\rm int}^{\overline{p}_{F_1}}(\widetilde{E}_5) \cup \mathcal{Z}_{\rm int}^{\overline{p}_{F_1}}(\widetilde{E}_9) \cup \{\widetilde{\nu}_5\}, \tag{5.31}$$

Next, we define the values of ϑ on the nodes of the edges $\widetilde{E}_1$ and $\widetilde{E}_6$, as well as on $\widetilde{\nu}_1$ and $\widetilde{\nu}_6$. We only consider $\widetilde{\nu}_1$ and $\widetilde{E}_1$ (the definition for $\widetilde{\nu}_6$ and $\widetilde{E}_6$ is completely analogous). If $\widetilde{\nu}_1 \in \mathcal{N}(\mathcal{T})$ (i.e., $\widetilde{\nu}_1$ is a hanging node of $\mathcal{T}$), then we define $\vartheta(z)$ for $z \in \mathcal{Z}_{\rm int}^{\overline{p}_{\widetilde{E}_1}}(\widetilde{E}_1) \cup \{\widetilde{\nu}_1\}$ by (5.24). If $\widetilde{\nu}_1 \notin \mathcal{N}(\mathcal{T})$, then $E_1 \in \mathcal{E}(\mathcal{T})$ and $\nu_1 \in \mathcal{N}(\mathcal{T})$. We

define $\vartheta(\nu_1)$ again by (5.24). Recall that $\vartheta(\nu_2) = \vartheta(\widetilde{\nu}_2)$ has already been defined. Then, for the nodes on $\widetilde{E}_1$, we set

$$\vartheta(z) = \vartheta(\nu_1)\Phi_K^{\nu_1}(z) + \vartheta(\nu_2)\Phi_K^{\nu_2}(z), \qquad z \in \mathcal{Z}_{\mathrm{int}}^{\overline{p}_{\widetilde{E}_1}}(\widetilde{E}_1) \cup \{\widetilde{\nu}_1\}. \tag{5.32}$$

Now we construct ϑ on $\widetilde{K}$ by setting

$$\begin{aligned}\vartheta(x) = &\sum_{\nu\in\mathcal{N}(\widetilde{K})} \vartheta(\nu)\ \Phi_{\widetilde{K}}^{\nu}(x) + \sum_{E\in\mathcal{E}(\widetilde{K})} \sum_{i=1}^{\overline{p}_E-1} \Big(\vartheta(z_i^{E,\overline{p}_E})\Phi_i^{E,\overline{p}_E}(x)\Big) \\ &+ \sum_{F\in\mathcal{F}(\widetilde{K})} \sum_{i,j=1}^{\overline{p}_F-1} \Big(\vartheta(z_{i,j}^{F,\overline{p}_F})\Phi_{i,j}^{F,\overline{p}_F}(x)\Big).\end{aligned} \tag{5.33}$$

This completes the construction of ϑ. It can be readily seen that $\vartheta \in S^{\mathrm{c}}_{\overline{p}}(\widetilde{\mathcal{T}})$.

We shall now derive an estimate analogous to (5.28) for Case 2. To do so, we estimate the difference between $v_{\widetilde{K}}$ and ϑ on $\widetilde{K}$ as follows:

$$\|v_{\widetilde{K}} - \vartheta\|_{L^2(\widetilde{K})} \lesssim \sum_{\widetilde{\nu}\in\mathcal{N}(\widetilde{K})} \|\varsigma_{\widetilde{\nu}}\|_{L^2(\widetilde{K})} + \sum_{\widetilde{E}\in\mathcal{E}(\widetilde{K})} \|\varsigma_{\widetilde{E}}\|_{L^2(\widetilde{K})} + \sum_{\widetilde{F}\in\mathcal{F}(\widetilde{K})} \|\varsigma_{\widetilde{F}}\|_{L^2(\widetilde{K})}, \tag{5.34}$$

with

$$\begin{aligned}\varsigma_{\widetilde{\nu}}(x) &= \big(v_{\widetilde{K}}(\widetilde{\nu}) - \vartheta(\widetilde{\nu})\big)\Phi_{\widetilde{K}}^{\widetilde{\nu}}(x), \\ \varsigma_{\widetilde{E}}(x) &= \sum_{i=1}^{\overline{p}_{\widetilde{E}}-1} \Big(\big(v_{\widetilde{K}}(z_i^{\widetilde{E},\overline{p}_{\widetilde{E}}}) - \vartheta(z_i^{\widetilde{E},\overline{p}_{\widetilde{E}}})\big)\ \Phi_i^{\widetilde{E},\overline{p}_{\widetilde{E}}}(x)\Big), \\ \varsigma_{\widetilde{F}}(x) &= \sum_{i,j=1}^{\overline{p}_{\widetilde{F}}-1} \Big(\big(v_{\widetilde{K}}(z_{i,j}^{\widetilde{F},\overline{p}_{\widetilde{F}}}) - \vartheta(z_{i,j}^{\widetilde{F},\overline{p}_{\widetilde{F}}})\big)\ \Phi_{i,j}^{\widetilde{F},\overline{p}_{\widetilde{F}}}(x)\Big).\end{aligned}$$

Proceeding as in the two-dimensional proof in [32, Lemma 5.4], we obtain the following estimates. First, we have that $\|\varsigma_{\widetilde{\nu}}\|_{L^2(\widetilde{K})} = 0$ for $\widetilde{\nu} \in \mathcal{N}_A(\widetilde{\mathcal{T}})$ and

$$\|\varsigma_{\widetilde{\nu}}\|_{L^2(\widetilde{K})} \lesssim \sum_{F\in w^F(\widetilde{\nu})} p_F^{-1} h_F^{1/2} \|[\![v]\!]\|_{L^2(F)}, \qquad \widetilde{\nu} \in \mathcal{N}(\mathcal{T}).$$

Second, for $\widetilde{\nu} \notin \mathcal{N}(\mathcal{T})$, we have

$$\|\varsigma_{\widetilde{\nu}}\|_{L^2(\widetilde{K})} \lesssim \begin{cases} \displaystyle\sum_{F\in\{w^F(\nu)\}_{\nu\in\partial E}} p_F^{-1} h_F^{1/2} \|[\![v]\!]\|_{L^2(F)}, & \exists\, E \in \mathcal{E}(K),\ \widetilde{\nu} \text{ is inside } E, \\ \displaystyle\sum_{F\in\{w^F(\nu)\}_{\nu\in\mathcal{N}(F^\star)}} p_F^{-1} h_F^{1/2} \|[\![v]\!]\|_{L^2(F)}, & \exists\, F^\star \in \mathcal{F}(K),\ \widetilde{\nu} \text{ inside } F^\star. \end{cases}$$

Similarly, for $\varsigma_{\widetilde{E}}$ in (5.34), we have that $\varsigma_{\widetilde{E}} = 0$ if $\widetilde{E} \in \mathcal{E}_A(\widetilde{\mathcal{T}})$ or if $\widetilde{E} \in \mathcal{E}_{F^\star}(K)$ for a face $F^\star \in \mathcal{F}_H(\mathcal{T}) \cap \mathcal{F}(K)$. Moreover, if $\widetilde{E} \in \mathcal{E}_{F^\star}(K)$ for a face $F^\star \in \mathcal{F}_N(\mathcal{T}) \cap \mathcal{F}(K)$, we have

$$\|\varsigma_{\widetilde{E}}\|_{L^2(\widetilde{K})} \lesssim \sum_{F\in\{w^F(\nu)\}_{\nu\in\mathcal{N}(F^\star)}} p_F^{-1} h_F^{1/2} \|[\![v]\!]\|_{L^2(F)}.$$

For the situation when there exists an edge $E \in \mathcal{E}(\mathcal{T})$ such that $\widetilde{E} \subseteq E$, we have

$$\|\varsigma_{\widetilde{E}}\|_{L^2(\widetilde{K})} \lesssim \sum_{F \in \{w^F(\nu)\}_{\nu \in \partial E}} p_F^{-1} h_F^{1/2} \|[\![v]\!]\|_{L^2(F)}.$$

Now we only need to bound $\|\varsigma_{\widetilde{F}}\|_{L^2(\widetilde{K})}$ in (5.34) for any face $\widetilde{F} \in \mathcal{F}(\widetilde{K})$. If $\widetilde{F} \in \mathcal{F}(\mathcal{T})$ or $\widetilde{F} \in \mathcal{F}_A(\widetilde{\mathcal{T}})$, by the construction of v and ϑ, we have $\|\varsigma_{\widetilde{F}}\|_{L^2(\widetilde{K})} = 0$. Otherwise, there exist a face $F \in \mathcal{F}(K)$ such that $F \in \mathcal{F}_R(\mathcal{T})$ and $\widetilde{F}$ is obtained by refining F. Without loss of generality, we may again consider the case illustrated in Figure 5.6, with the faces F and $\widetilde{F}$ discussed being F_1 and $\widetilde{F}_1$, respectively. If $F_1 \in \mathcal{F}_H(\mathcal{T})$, then $\|\varsigma_{\widetilde{F}_1}\|_{L^2(\widetilde{K})} = 0$. Otherwise, $F_1 \in \mathcal{F}_N(\mathcal{T})$. Since $\varsigma_{\widetilde{F}_1}$ vanishes at all the interior tensor-product Gauss-Lobatto nodes in $\widetilde{K}$ and on the faces of $\mathcal{Z}_{\rm int}^{p_{\widetilde{K}}}(\widetilde{K})$ that are different from $\widetilde{F}_1$, we obtain from Lemma 5.1(i) and the construction of v and ϑ that

$$\begin{aligned}
&\|\varsigma_{\widetilde{F}_1}\|_{L^2(\widetilde{K})} \lesssim p_{\widetilde{K}}^{-1} h_{\widetilde{K}}^{1/2} \|\varsigma_{\widetilde{F}_1}\|_{L^2(\widetilde{F}_1)} \\
&\lesssim p_{\widetilde{K}}^{-1} h_{\widetilde{K}}^{1/2} \big(\|v_{\widetilde{K}} - \vartheta\|_{L^2(\widetilde{F}_1)} + \sum_{i \in \{1,5,6,9\}} \|\varsigma_{\widetilde{E}_i}\|_{L^2(\widetilde{F}_1)} + \sum_{j \in \{1,2,5,6\}} \|\varsigma_{\widetilde{\nu}_j}\|_{L^2(\widetilde{F}_1)} \big) \\
&\lesssim p_K^{-1} h_K^{1/2} \|v_{\widetilde{K}} - \vartheta\|_{L^2(F_1)} + p_K^{-1} h_K^{1/2} \big(\sum_{i \in \{1,5,6,9\}} \|\varsigma_{\widetilde{E}_i}\|_{L^2(\widetilde{F}_1)} + \sum_{j \in \{1,2,5,6\}} \|\varsigma_{\widetilde{\nu}_j}\|_{L^2(\widetilde{F}_1)} \big) \\
&\equiv T_1 + T_2.
\end{aligned}$$

Using (5.27), Lemma 5.1(iii) and (2.3), we get

$$\begin{aligned}
T_1 &\lesssim p_K^{-1} h_K^{1/2} \sum_{\nu \in \mathcal{N}(F_1)} \|\varsigma_\nu\|_{L^2(F_1)} \lesssim p_K^{-1} h_K^{1/2} \sum_{\nu \in \mathcal{N}(F_1)} \big(|v_K(\nu) - \vartheta(\nu)| \, \|\Phi_K^\nu\|_{L^2(F_1)} \big) \\
&\lesssim \sum_{F \in \{w^F(\nu)\}_{\nu \in \mathcal{N}(F_1)}} p_F^{-1} h_F^{1/2} \|[\![v]\!]\|_{L^2(F)}.
\end{aligned}$$

In an analogous manner to the two-dimensional proof in [32, Lemma 5.4], term T_2 is bounded by

$$T_2 \lesssim \sum_{F \in \{w^F(\nu)\}_{\nu \in \mathcal{N}(F_1)}} p_F^{-1} h_F^{1/2} \|[\![v]\!]\|_{L^2(F)}.$$

Hence, $\varsigma_{\widetilde{F}}$ in (5.34) can be bounded by

$$\|\varsigma_{\widetilde{F}}\|_{L^2(\widetilde{K})} \lesssim \sum_{F \in \{w^F(\nu)\}_{\nu \in \mathcal{N}(F_1)}} p_F^{-1} h_F^{1/2} \|[\![v]\!]\|_{L^2(F)}.$$

To combine the bounds for $\varsigma_{\widetilde{\nu}}$, $\varsigma_{\widetilde{E}}$ and $\varsigma_{\widetilde{F}}$, we define the set $\mathcal{N}^\star(\widetilde{K})$ as follows. We start from $\mathcal{N}(\widetilde{K})$ and first remove all the vertices belonging to $\mathcal{N}_A(\widetilde{\mathcal{T}})$. Then, any vertex $\widetilde{\nu} \in \mathcal{N}(\widetilde{K})$ with $\widetilde{\nu} \notin \mathcal{N}(\mathcal{T}) \cup \mathcal{N}_A(\widetilde{\mathcal{T}})$ is replaced by the vertex $\nu \in \mathcal{N}(K)$ which lies on the same elemental edge of K as $\widetilde{\nu}$; see [32, Section 5.5]. We also set

$$\mathcal{F}^\star(\widetilde{K}) = \{ \, F \in w^F(\nu) \, : \, \nu \in \mathcal{N}^\star(\widetilde{K}) \, \}.$$

Thus, we have

$$\|v_{\widetilde{K}} - \vartheta\|_{L^2(\widetilde{K})} \lesssim \sum_{F \in \mathcal{F}^\star(\widetilde{K})} p_F^{-1} h_F^{1/2} \|[\![v]\!]\|_{L^2(F)}. \tag{5.35}$$

This completes the discussion of Case 2.

By the key estimates in (5.28) and (5.35), we have in both cases above

$$\|v_{\widetilde{K}} - \vartheta\|_{L^2(\widetilde{K})} \lesssim \sum_{F\in\mathcal{F}^\star(\widetilde{K})} p_F^{-1} h_F^{1/2} \|[\![v]\!]\|_{L^2(F)}, \qquad \widetilde{K}\in\widetilde{\mathcal{T}}. \tag{5.36}$$

This proves the first inequality in (5.20). Moreover, by the inverse inequality,

$$\|\nabla v\|_{L^2(\widetilde{K})} \lesssim p_{\widetilde{K}}^2 h_{\widetilde{K}}^{-1} \|v\|_{L^2(\widetilde{K})}, \qquad v\in S_{\underline{\widetilde{p}}}(\widetilde{\mathcal{T}}),\ \widetilde{K}\in\widetilde{\mathcal{T}}, \tag{5.37}$$

see [10], we obtain from (5.36) and (2.3)

$$\|\nabla(v_{\widetilde{K}} - \vartheta)\|_{L^2(\widetilde{K})} \lesssim \sum_{F\in\mathcal{F}^\star(\widetilde{K})} p_F h_F^{-1/2} \|[\![v]\!]\|_{L^2(F)}, \qquad \widetilde{K}\in\widetilde{\mathcal{T}}, \tag{5.38}$$

which shows the second assertion in the nodal approximation result (5.20).

5.7.2. Edge approximation. For any edge $E\in\mathcal{E}(\mathcal{T})$, we define the set

$$w_E = \{\, K\in\mathcal{T} \,:\, E\subset\partial K \,\}. \tag{5.39}$$

Fix an element $K\in\mathcal{T}$. First, we consider an elemental edge $E\in\mathcal{E}(K)$ and define the function W_K^E as follows: if $E\in\mathcal{E}_B(\mathcal{T})$, we set

$$W_K^E = L^E_{p_K,K}\big((v_K - v_K^{\rm nod})|_E\big),$$

with the extension operator $L^E_{p_K,K}(\cdot)$ defined in (5.2).

If $E\in\mathcal{E}_I(\mathcal{T})$, let $K'\in w_E$ be the element which has the lowest polynomial degree in the set w_E defined in (5.39); see [32, Section 5.6]. We define W_K^E by

$$W_K^E = L^E_{p_K,K}\big((v_{K'} - v_{K'}^{\rm nod})|_E\big),$$

with $L^E_{p_K,K}(\cdot)$ defined in (5.2).

In the case where E contains a hanging node, E is partitioned into $E=E_1\cup E_2$ with $E_1,E_2\in\mathcal{E}_I(\mathcal{T})$, cf. Figure 5.2. Denote by $K'\in w_{E_1}$ and $K''\in w_{E_2}$ the elements in $\mathcal{T}$ which have the lowest polynomial degree in the set w_{E_1} and w_{E_2}, respectively; see [32, Section 5.6]. We now define W_K^E by

$$W_K^E = L^E_{p_K,K}\big((v_{K'} - v_{K'}^{\rm nod})|_{E_1}, (v_{K''} - v_{K''}^{\rm nod})|_{E_2}\big),$$

with $L^E_{p_K,K}(\cdot,\cdot)$ in (5.3).

Next, for an edge $E\in\mathcal{E}_F(K)$, $F\in\mathcal{F}(K)$, the function W_K^E is given analogously. Let $K'\in w_E$ be the element which has the lowest polynomial degree in the set w_E. We define W_K^E by

$$W_K^E = L^E_{p_K,K}\big((v_{K'} - v_{K'}^{\rm nod})|_E\big),$$

with $L^E_{p_K,K}(\cdot)$ given in (5.5).

Then we define $\vartheta^{\rm edge}$ elementwise by setting

$$\vartheta^{\rm edge}|_K = \sum_{E\in\mathcal{E}(K)} W_K^E + \sum_{F\in\mathcal{F}(K)}\sum_{E\in\mathcal{E}_F(K)} W_K^E,$$

with W_K^E defined above. Clearly, the function $\vartheta^{\rm edge}$belongs to $S^c_{\underline{\widetilde{p}}}(\widetilde{\mathcal{T}})$. By employing Lemma 5.2 and proceeding as in [32, Section 5.6], the approximation property (5.21) can be readily derived.

5.7.3. Face approximation. Fix an element $K \in \mathcal{T}$ and let F be an element face in $\mathcal{F}(K)$. We define the function W_K^F as follows: if $F \in \mathcal{F}_B(\mathcal{T})$, we set

$$W_K^F = L_{p_K,K}^F\big((v_K - v_K^{\mathrm{nod}} - v_K^{\mathrm{edge}})|_F\big),$$

with $L_{p_K,K}^F(\cdot)$ defined in (5.6). If $F \in \mathcal{F}_I(\mathcal{T})$, let K' in $\mathcal{T}$ be the neighboring element such that $F \in \mathcal{F}(K) \cap \mathcal{F}(K')$. Denote by $\underline{K}'$ the element which has the lower polynomial degree of the elements K and K'. We define W_K^F by

$$W_K^F = L_{p_K,K}^F\big((v_{\underline{K}'} - v_{\underline{K}'}^{\mathrm{nod}} - v_{\underline{K}'}^{\mathrm{edge}})|_F\big),$$

with $L_{p_K,K}^F(\cdot)$ defined in (5.8) if $F \in \mathcal{F}_H(\mathcal{T})$ (see Figure 5.5) and in (5.6) otherwise. If F contains a hanging node in the center, F is partitioned into $F = \cup_{i=1}^4 F_i$ with $F_i \in \mathcal{F}(\mathcal{T})$, $i = 1, \ldots, 4$, cf. Figure 5.4. There exist four elements $K_i \in \mathcal{T}$ such that $F_i \in \mathcal{F}(K_i)$. Denote by $\underline{K}_i$ the element that has the lower polynomial degree of K and K_i, $i = 1, \ldots, 4$. We now define W_K^F by

$$W_K^F = L_{p_K,K}^F\big((v_{\underline{K}_1} - v_{\underline{K}_1}^{\mathrm{nod}} - v_{\underline{K}_1}^{\mathrm{edge}})|_{F_1}, \ldots, (v_{\underline{K}_4} - v_{\underline{K}_4}^{\mathrm{nod}} - v_{\underline{K}_4}^{\mathrm{edge}})|_{F_4}\big),$$

with $L_{p_K,K}^F(\cdot,\cdot,\cdot,\cdot)$ defined in (5.7).

Next, we prove the face approximation property (5.22). By (2.3), Lemma 5.3 and the polynomial trace inequality (see [29]), we have

$$\begin{aligned}
\sum_{\widetilde{K}\in\widetilde{\mathcal{T}}} \|v^{\mathrm{face}} - \vartheta^{\mathrm{face}}\|_{L^2(\widetilde{K})}^2 &= \sum_{K\in\mathcal{T}} \sum_{\widetilde{K}\in\mathcal{R}(K)} \|v^{\mathrm{face}} - \vartheta^{\mathrm{face}}\|_{L^2(\widetilde{K})}^2 \\
&\lesssim \sum_{K\in\mathcal{T}} \sum_{F\in\mathcal{F}(K)} \|L_{p_K,K}^F\big((v_K - v_K^{\mathrm{nod}} - v_K^{\mathrm{edge}})|_F\big) - W_K^F\|_{L^2(K)}^2 \\
&\lesssim \sum_{K\in\mathcal{T}} \sum_{F\in\mathcal{F}(K)} p_K^{-2} h_K \|(v_K - v_K^{\mathrm{nod}} - v_K^{\mathrm{edge}})|_F - W_K^F|_F\|_{L^2(F)}^2 \\
&\lesssim \sum_{K\in\mathcal{T}} \sum_{F\in\mathcal{F}(K)} p_F^{-2} h_F (\|[\![v]\!]\|_{L^2(F)}^2 + \|[\![v^{\mathrm{nod}}]\!]\|_{L^2(F)}^2 + \|[\![v^{\mathrm{edge}}]\!]\|_{L^2(F)}^2) \\
&\lesssim \sum_{K\in\mathcal{T}} \sum_{F\in\mathcal{F}(K)} p_F^{-2} h_F (\|[\![v]\!]\|_{L^2(F)}^2 + \|[\![v^{\mathrm{nod}}]\!]\|_{L^2(F)}^2) + \sum_{\widetilde{K}\in\widetilde{\mathcal{T}}} \|[\![v^{\mathrm{edge}}]\!]\|_{L^2(\widetilde{K})}^2.
\end{aligned}$$

This, together with the edge approximation result (5.21) completes the proof of the first assertion of (5.22); the second one follows again from the first one by using the inverse inequality in (5.37).

6. Numerical experiments. In this section, we present a series of numerical examples to demonstrate the practical performance of the proposed a-posteriori error estimator η derived in Theorem 3.1 within an automatic *hp*-adaptive refinement procedure which is based on 1-irregular hexahedral elements. In each of the examples shown in this section the DG solution u_{hp} defined by (2.6) is computed with the interior penalty parameter γ equal to 10. All computations have been performed using the `AptoFEM` software package (see [14], for details). Additionally, the resulting system of linear equations is solved by exploiting the MUltifrontal Massively Parallel Solver (MUMPS), see [1, 2, 3], for example.

The *hp*-adaptive meshes are constructed by first marking the elements for refinement according to the size of the local error indicators η_K; this is achieved by

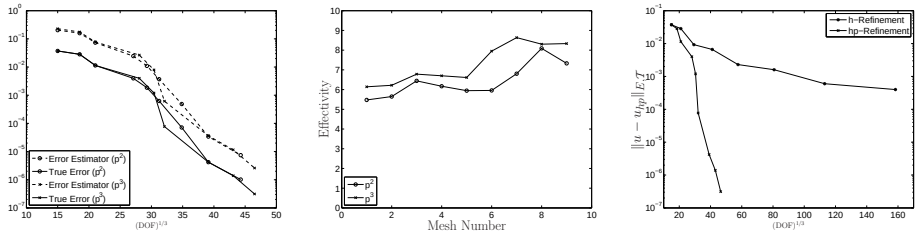

(a) (b) (c)

FIG. 6.1. Example 1. *(a) Comparison of the actual and estimated energy norm of the error with respect to the (third root of the) number of degrees of freedom with hp-adaptive mesh refinement; (b) Effectivity indices; (c) Comparison of the actual error with h- and hp-adaptive mesh refinement.*

employing the fixed fraction strategy, see [19], with refinement fraction 25%. Note that in the present article, we do not employ any derefinement of the underlying *hp*-meshes. Once an element $K \in \mathcal{T}$ has been flagged for refinement, a decision must be made whether the local mesh size h_K or the local degree p_K of the approximating polynomial should be adjusted accordingly. The choice to perform either *h*- or *p*-refinement is based on estimating the local smoothness of the (unknown) analytical solution. To this end, we employ the *hp*-adaptive strategy developed in [20], where the local regularity of the analytical solution is estimated from truncated local Legendre expansions of the computed numerical solution; see, also, [12, 18].

Here, the emphasis will be on investigating the asymptotic sharpness of the proposed a-posteriori error bound on a sequence of nonuniform *hp*-adaptively refined 1-irregular meshes. To this end, we shall compare the estimator η derived in Theorem 3.1, which is slightly suboptimal (by a factor of $p_F^{1/2}$) in the face polynomial order p_F, with the indicator $\widehat{\eta}$ discussed in Remark 3.2; we note that the derivation of the latter precludes the use of hanging nodes, at least theoretically. Indeed, here we shall show that despite the loss of optimality in the polynomial degree, both indicators perform extremely well on *hp*-refined meshes, in the sense that the *effectivity index*, which is defined as the ratio of the a-posteriori error bound and the energy norm of the actual error, is roughly constant on all of the meshes employed. Moreover, our numerical experiments indicate that both a-posteriori error indicators give rise to very similar quantitative results. For simplicity, as in [7], we set the constant C arising in Theorem 3.1 equal to one; in general, to ensure the reliability of the error estimator, this constant must be determined numerically for the underlying problem at hand. In all of our experiments, the data-approximation terms in the a-posteriori bound stated in Theorem 3.1 will be neglected. For both the error estimators η and $\widehat{\eta}$, inhomogeneous boundary conditions are incorporated as discussed in Remark 3.4.

6.1. Example 1. In this example, we let Ω be the unit cube $(0,1)^3$ in $\mathbb{R}^3$; further, we select f and an appropriate inhomogeneous boundary condition, so that the analytical solution to (1.1) is given by

$$u(x_1, x_2, x_3) = \sin(\pi x_1)\cos(\pi x_2)\cos(\pi x_3).$$

In Figure 6.1(a) we present a comparison of the actual and estimated energy norm of the error versus the third root of the number of degrees of freedom in the finite element space $S_{\underline{p}}(\mathcal{T})$ on a linear-log scale, for the sequence of meshes generated by our *hp*-adaptive algorithm using the indicator η stated in Theorem 3.1 (denoted by p^3 in

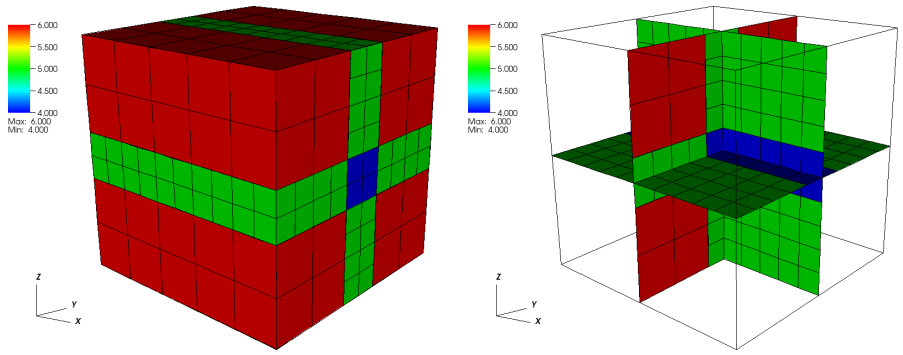

FIG. 6.2. Example 1. *Finite element mesh after* 8 *adaptive refinements, with* 440 *elements and* 100578 *degrees of freedom: (a) hp-mesh; (b) Three-slice of the hp-mesh.*

the figure) and $\widehat{\eta}$ outlined in Remark 3.2 (denoted by p^2). Here, we observe that the two error indicators perform in a very similar manner: in each case the error bound over-estimates the true error by a (reasonably) consistent factor. From Figure 6.1(b), we see that the computed effectivity indices lie in the range 5–9; in particular, we note that although there is some initial growth in the effectivity indices as the *hp*-mesh is refined, these numbers seem to settle at approximately 8 as the adaptive refinement strategy proceeds. Additionally, from Figure 6.1(a) we observe that after an initial transient, the convergence lines using *hp*-refinement are (roughly) straight on a linear-log scale, which indicates that exponential convergence is attained for this smooth problem, as we would expect. In Figure 6.1(c), we present a comparison between the actual energy norm of the error employing both *h*- and *hp*-mesh refinement; here, the *hp*-refinement is based on employing the error indicator stated in Theorem 3.1. In the former case, the DG solution u_{hp} is computed using triquadratic elements, i.e., $p_K = 2$; here, the adaptive algorithm is again based on employing the fixed fraction strategy, with the refinement fraction set to 25%, without any derefinement. From Figure 6.1(c), we clearly observe the superiority of employing a grid adaptation strategy based on exploiting *hp*-adaptive refinement: on the final mesh, the energy norm of the error using *hp*-refinement is around four orders of magnitude smaller than the corresponding quantity computed when *h*-refinement is employed alone.

In Figure 6.2 we show the mesh generated using the proposed *hp*-version a-posteriori error indicator stated in Theorem 3.1 after 8 *hp*-adaptive refinement steps. For clarity, we also show the three-slice of the *hp*-mesh centered at the centroid of the computational domain Ω. Here, we observe that some *h*-refinement of the mesh has been performed in the vicinity of steep gradients present in the analytical solution situated in the interior of Ω. Within this region, the polynomial degree is between 4–5. Away from this region, the *hp*-adaptive algorithm increases the degree of the approximating polynomial where the analytical solution is extremely smooth.

6.2. Example 2. In this section, we let Ω be the Fichera corner $(-1,1)^3 \setminus [0,1)^3$, and select f and an appropriate inhomogeneous boundary condition for u so that

$$u(x_1, x_2, x_3) = (x_1^2 + x_2^2 + x_3^2)^{q/2},$$

where q is a real number. We note that for $q > -1/2$, the analytical solution u to (1.1) satisfies $u \in H^1(\Omega)$; cf. [8], for example. In this section we set $q = -1/4$; in this case u

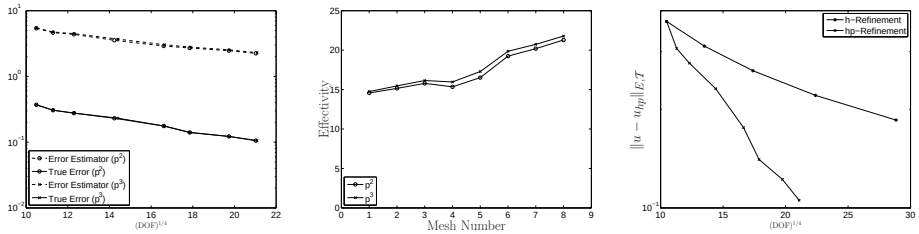

(a) (b) (c)

FIG. 6.3. Example 2. *(a) Comparison of the actual and estimated energy norm of the error with respect to the (fourth root of the) number of degrees of freedom with hp-adaptive mesh refinement; (b) Effectivity indices; (c) Comparison of the actual error with h- and hp-adaptive mesh refinement.*

possesses typical (isotropic) singular behavior that solutions of elliptic boundary-value problems exhibit in the vicinity of reentrant corners in the computational domain. The most general type of singularity involving anisotropic edge singularities will be treated elsewhere.

Figure 6.3(a) shows the history of the actual and estimated energy norm of the error on each of the meshes generated by our *hp*-adaptive algorithm using both the indicator η in Theorem 3.1 (denoted by p^3 in the figure) and $\widehat{\eta}$ in Remark 3.2 (denoted by p^2). Here, we have plotted the errors versus the fourth root of the number of degrees of freedom in the finite element space $S_{\underline{p}}(\mathcal{T})$ on a linear-log scale; the fourth root of the number of degrees of freedom is chosen empirically based on the fact that the singularity is isotropic; we also refer to the two–dimensional *hp*-version a-priori error analysis performed in [30]. We point out that for general (anisotropic) edge singularities in 3D, the fifth root of the degrees of freedom should be considered; cf. [27].

As in the previous example, we observe that the two error indicators perform in a very similar manner, though for this non-smooth example the loss in optimality in the jump indicator in the estimator stated in Theorem 3.1 does lead to a slight increase in the effectivity indices in comparison with indicator $\widehat{\eta}$ in (3.6). Indeed, from Figure 6.3(b) we observe that the effectivity indices for both a-posteriori bounds do slowly grow as the *hp*-mesh is refined. Additionally, from Figure 6.3(a) we observe exponential convergence of the energy norm of the error using both estimators with *hp*-refinement; indeed, on a linear-log scale, the convergence lines are, on average, straight. Figure 6.3(c) highlights the superiority of employing *hp*-adaptive refinement in comparison with *h*-refinement. Indeed, although on the final mesh, the energy norm of the error using the *hp*-refinement indicator stated in Theorem 3.1 is only around a factor 2 smaller than the corresponding quantity when *h*-refinement is employed alone, based on using triquadratic elements, we can clearly see that an excessively large number of degrees of freedom will be required to simply ensure that $\|u-u_{hp}\|_{E,\mathcal{T}}$ is less than 10^{-1} when using the fixed-order *h*-refinement strategy.

In Figure 6.4 we show the mesh generated using the local error indicators η_K stated in Theorem 3.1 after 7 *hp*-adaptive refinement steps. Here, we see that the *h*-mesh has been refined in the vicinity of the re-entrant corner located at the origin. Additionally, we see that the polynomial degrees have been increased away from the re-entrant corner located at the origin, since the underlying analytical solution is smooth in this region.

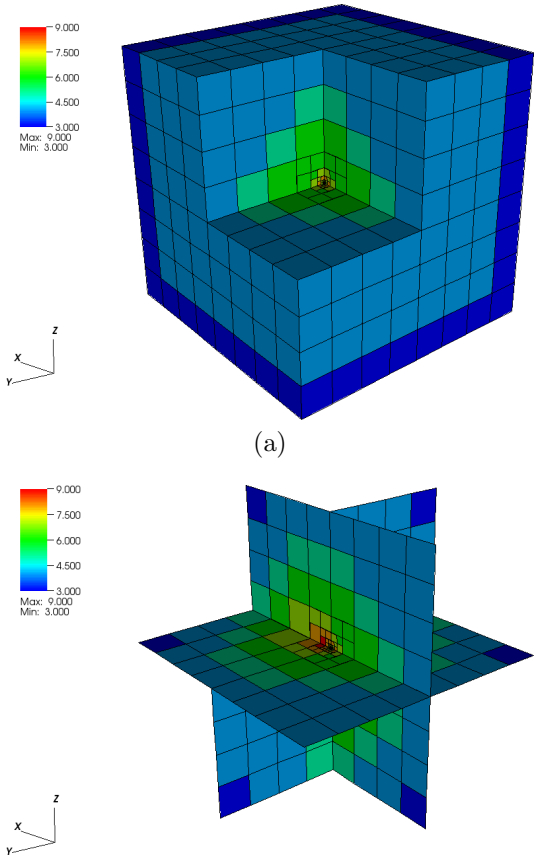

FIG. 6.4. Example 2. *Finite element mesh after* 7 *adaptive refinements, with* 686 *elements and* 197670 *degrees of freedom: (a) hp-mesh; (b) Three-slice of the hp-mesh.*

7. Conclusions. In this paper, we derived an a-posteriori error estimator for *hp*-adaptive DG methods for elliptic problems on 1-irregularly, isotropically refined meshes in three dimensions. The estimator yields upper and lower bounds for the error measured in terms of the natural energy norm. We applied our estimate as an error indicator for energy norm error estimation in an *hp*-adaptive refinement algorithm. Our numerical results show that the indicator is efficient in locating and resolving isotropic corner singularities at exponential convergence rates.

In our analysis, we employed the approximation properties of the three-dimensional *hp*-version averaging operator in Theorem 4.1. This theorem allows us to also extend the analysis in [32] to three dimensions. Hence, a robust a-posteriori error estimator for *hp*-adaptive DG discretizations of three-dimensional stationary convection-diffusion equations can be immediately obtained. As in [32], such an estimator yields global upper and lower bounds of the errors measured in terms of the natural energy norm associated with the diffusion and a semi-norm associated with the convection. In particular, the constants are independent of the Péclet number of the problem.

Acknowledgements. LZ and DS were supported in part by the Natural Sciences and Engineering Research Council of Canada (NSERC). SG and PH acknowledge the

financial support of the European Union, under the ADIGMA project.

REFERENCES

[1] P. R. Amestoy, I. S. Duff, J. Koster, and J.-Y. L'Excellent. A fully asynchronous multifrontal solver using distributed dynamic scheduling. *SIAM Journal on Matrix Analysis and Applications*, 23:15–41, 2001.

[2] P. R. Amestoy, I. S. Duff, and J.-Y. L'Excellent. Multifrontal parallel distributed symmetric and unsymmetric solvers. *Comput. Methods Appl. Mech. Eng.*, 184:501–520, 2000.

[3] P. R. Amestoy, A. Guermouche, J.-Y. L'Excellent, and S. Pralet. Hybrid scheduling for the parallel solution of linear systems. *Parallel Computing*, 32:136–156, 2006.

[4] D.N. Arnold. An interior penalty finite element method with discontinuous elements. *SIAM J. Numer. Anal.*, 19:742–760, 1982.

[5] D.N. Arnold, F. Brezzi, B. Cockburn, and L.D. Marini. Unified analysis of discontinuous Galerkin methods for elliptic problems. *SIAM J. Numer. Anal.*, 39:1749–1779, 2002.

[6] C.E. Baumann and J.T. Oden. A discontinuous *hp*-finite element method for convection-diffusion problems. *Comput. Methods Appl. Mech. Engrg.*, 175:311–341, 1999.

[7] R. Becker, P. Hansbo, and M.G. Larson. Energy norm a posteriori error estimation for discontinuous Galerkin methods. *Comput. Methods Appl. Mech. Engrg.*, 192:723–733, 2003.

[8] L. Beilina, S. Korotov, and M. Křížek. Nonobtuse tetrahedral partitions that refine locally towards Fichera-like corners. *App. Math.*, 50:569–581, 2005.

[9] E. Burman and A. Ern. Continuous interior penalty *hp*-finite element methods for advection and advection-diffusion equations. *Math. Comp.*, 76:1119–1140, 2007.

[10] C. Canuto and A. Quarteroni. Approximation results for orthogonal polynomials in Sobolev spaces. *Math. Comp.*, 38:67–86, 1982.

[11] B. Cockburn, G.E. Karniadakis, and C.-W. Shu. The development of discontinuous Galerkin methods. In B. Cockburn, G.E. Karniadakis, and C.-W. Shu, editors, *Discontinuous Galerkin Methods: Theory, Computation and Applications*, volume 11 of *Lect. Notes Comput. Sci. Engrg.*, pages 3–50. Springer–Verlag, 2000.

[12] T. Eibner and J. M. Melenk. An adaptive strategy for *hp*-FEM based on testing for analyticity. *Comp. Mech.*, 39:575–595, 2007.

[13] A. Ern and A.F. Stephansen. A posteriori energy-norm error estimates for advection-diffusion equations approximated by weighted interior penalty methods. *J. Comp. Math.*, 26:488–510, 2008.

[14] S. Giani, E.J.C. Hall, and P. Houston. `AptoFEM`: Users manual. Technical report, University of Nottingham. In preparation.

[15] P. Houston, D. Schötzau, and T. Wihler. An *hp*-adaptive discontinuous Galerkin FEM for nearly incompressible linear elasticity. *Comput. Methods Appl. Mech. Engrg.*, 195:3224–3246, 2006.

[16] P. Houston, D. Schötzau, and T. P. Wihler. Energy norm a-posteriori error estimation of *hp*-adaptive discontinuous Galerkin methods for elliptic problems. *Math. Models Methods Appl. Sci.*, 17:33–62, 2007.

[17] P. Houston, C. Schwab, and E. Süli. Discontinuous *hp*-finite element methods for advection–diffusion–reaction problems. *SIAM J. Numer. Anal.*, 39:2133–2163, 2002.

[18] P. Houston, B. Senior, and E. Süli. Sobolev regularity estimation for *hp*–adaptive finite element methods. In F. Brezzi, A. Buffa, S. Corsaro, and A. Murli, editors, *Numerical Mathematics and Advanced Applications ENUMATH 2001*, pages 631–656. Springer, 2003.

[19] P. Houston and E. Süli. Adaptive finite element approximation of hyperbolic problems. In T. Barth and H. Deconinck, editors, *Error Estimation and Adaptive Discretization Methods in Computational Fluid Dynamics. Lect. Notes Comput. Sci. Engrg.*, volume 25, pages 269–344. Springer–Verlag, 2002.

[20] P. Houston and E. Süli. A note on the design of *hp*–adaptive finite element methods for elliptic partial differential equations. *Comput. Methods Appl. Mech. Engrg.*, 194:229–243, 2005.

[21] P. Houston, E. Süli, and T. Wihler. A-posteriori error analysis of *hp*-version discontinous Galerkin finite-element methods for second-order quasi-linear elliptic PDEs. *IMA J. Numer. Anal.*, 28:245–273, 2008.

[22] O. A. Karakashian and F. Pascal. A-posteriori error estimates for a discontinuous Galerkin approximation of second-order elliptic problems. *SIAM J. Numer. Anal.*, 41:2374–2399, 2003.

[23] J.M. Melenk and B.I. Wohlmuth. On residual-based a-posteriori error estimation in *hp*-FEM. *Adv. Comp. Math.*, 15:311–331, 2001.

[24] J. Nitsche. Über ein Variationsprinzip zur Lösung von Dirichlet Problemen bei Verwendung von Teilräumen, die keinen Randbedingungen unterworfen sind. *Math. Abh. Sem. Univ. Hamburg*, 36:9–15, 1971.

[25] I. Perugia and D. Schötzau. An *hp*-analysis of the local discontinuous Galerkin method for diffusion problems. *J. Sci. Comp.*, 17:561–571, 2002.

[26] B. Rivière, M.F. Wheeler, and V. Girault. Improved energy estimates for interior penalty, constrained and discontinuous Galerkin methods for elliptic problems, Part I. *Computational Geosciences*, 3:337–360, 1999.

[27] D. Schötzau, C. Schwab, and T. Wihler. Exponential convergence of *hp*-DGFEM for linear second-order elliptic problems in polyhedra. *In preparation*.

[28] D. Schötzau and L. Zhu. A robust a-posteriori error estimator for discontinuous Galerkin methods for convection-diffusion equations. *Appl. Numer. Math.*, 59:2236–2255, 2009.

[29] C. Schwab. *p- and hp-Finite Element Methods -Theory and Application to Solid and Fluid Mechanics*. Oxford University Press, Oxford, 1998.

[30] T. Wihler, P. Frauenfelder, and C. Schwab. Exponential convergence of the *hp*-DGFEM for diffusion problems. *Comput. Math. Appl.*, 46:183–205, 2003.

[31] L. Zhu. *Robust a-posteriori error estimation for discontinuous Galerkin methods for convection-diffusion equations*. PhD thesis, University of British Columbia, 2010.

[32] L. Zhu and D. Schötzau. A robust a-posteriori error estimate for *hp*-adaptive DG methods for convection-diffusion equations. *IMA J. Numer. Anal.*, to appear.